an association with histologic type most likely are false-positive results. In our analysis of *$ALDH_2$*, the incidence of adenocarcinoma was high among individuals who had the wild-type genotype. Although a high incidence of squamous cell carcinoma was not observed, this result may imply that carcinogenesis caused by acetaldehyde occurs more in cancers other than adenocarcinoma as well as in esophageal and upper aerodigestive tract cancers.

A previous hospital-based study that was conducted in Japan failed to identify any association between the *RsaI* polymorphism and lung cancer, even when the analysis was stratified according to different histologic type.[28] A more recent study indicated that there was a significant decrease in overall lung cancer risk associated with the possession of at least 1 copy of the *CYP2E1 RsaI* variant allele, whereas there was no association between the *CYP2E1 RsaI* polymorphism and the histologic type of lung cancer.[27] However, none of the previous studies had adjusted for risk according to alcohol consumption levels, which strongly influence the activity of this enzyme. In the current study, we demonstrated that there is a difference between individuals who have the *CYP2E1 RsaI* c2/c2 genotype compared with individuals who have the common c1/c1 genotype, with an adjusted OR of 4.66 (95% CI, 1.36–16.0) for the former group. Because of the low incidence of homozygosity in controls, the genotype distribution was not in Hardy-Weinberg equilibrium in our control population. The increased lung cancer risk among individuals with the *CYP2E1* c2/c2 genotype likely was a false-positive result.

A correlation between the amount of alcohol consumed, genetic polymorphisms in the alcohol metabolite-related enzymes, and the stage of lung cancer was not observed in the current study, and we could not confirm that these factors were related to the aggressiveness of lung cancer. Furthermore, no associations were identified between the location of the primary cancer, the amount of alcohol consumed, and the genotype of these enzymes or between the risk for lung cancer and the type of alcoholic beverage consumed.

In summary, we report a significant association between amounts of alcohol consumed and susceptibility to lung cancer and that the risk of lung cancer in individuals with *$ALDH_2$* variant alleles, but not with *ADH_3* or *CYP2E1* variant alleles, apparently was enhanced more by alcohol intake than in individuals with common genotypes. Moreover, to our knowledge, this is the first report documenting an association between lung cancer and genetic polymorphisms of alcohol metabolite-related enzymes. Because the sample size was relatively small for the investigation of effects stratified by each genotype, the current findings should be confirmed in large-scale studies with greater statistical power.

REFERENCES

1. Bandera EV, Freudenheim JL, Vena JE. Alcohol consumption and lung cancer: a review of the epidemiologic evidence. *Cancer Epidemiol Biomarkers Prev.* 2001;10:813–821.
2. Glade MJ. Food, Nutrition and the Prevention of Cancer: A Global Perspective. American Institute for Cancer Research. *Nutrition.* 1999;6:523–526.
3. Bagnardi V, Blangiardo M, La Vecchia C, Corrao G. A meta-analysis of alcohol drinking and cancer risk. *Br J Cancer.* 2001;85:1700–1705.
4. International Agency for Research on Cancer. Allyl compounds, aldehyde, epoxies and peroxidies. *IARC Monogr Eval Carcinog Risks Hum.* 1985;36:101–132.
5. Delanco VL. A mutagenicity assessment of acetaldehyde. *Mutat Res.* 1998;195:1–20.
6. Helander A, Lindahl-Keissling K. Increased frequency of acetaldehyde-induced sister chromatic exchanges in human lymphocytes treated with an aldehyde dehydrogenase inhibitor. *Mutat Res.* 1991;264:103–107.
7. Woutersen RA, Applman LM, Van Garderen-Hoetmer A, Feron VJ. Inhalation toxicity of acetaldehyde in rat. III. Carcinogenicity study. *Toxicology.* 1986;41:213–231.
8. Feron VJ, Kruysse A, Woutersen RA. Respiratory tract tumors in hamsters exposed to acetaldehyde vapour alone or simultaneously to benzo[a]pyrene or diethylnitrosamine. *Eur J Cancer Clin Oncol.* 1982;18:13–31.
9. Kunitoh S, Imaoka S, Hiroi T, Yabusaki Y, Monna T, Funae Y. Acetaldehyde as well as ethanol is' metabolized by human CYP2E1. *Pharmacol Exp Ther.* 1997;280:527–532.
10. Liber CS, DeCarli LM. Hepatic microsomal ethanol oxidizing system. *J Biol Chem.* 1970;254:2505–2512.
11. Bosron WF, Li TK. Genetic polymorphisms of human liver alcohol and aldehyde dehydrogenases and their relationship to alcohol metabolism and alcoholism. *Hepatology.* 1986;6:502–510.
12. Harada S, Misawa S, Agarwal DP, Goedde HW. Liver alcohol dehydrogenase and aldehyde dehydrogenase in Japanese: isozyme variation and its possible role in alcohol intoxication. *Am J Hum Genet.* 1980;32:8–15.
13. Sun F, Tsuritani I, Yamada Y. Contribution of genetic polymorphisms in ethanol-metabolizing enzymes to problem drinking behavior in middle-aged Japanese men. *Behav Genet.* 2002;32:229–236.
14. Iwahashi K, Miyatake R, Suwaki H, et al. Blood ethanol levels and the CYP2E1 C2 allele. *Arukoru Kenkyuto Yakubutsu Ison.* 1994;29:190–194.
15. Hayashi S, Watanabe J, Kawajiri K. Genetic polymorphism in 5'-flanking region change transcriptional regulation of the human cytochrome P-450IIE1 gene. *J Biochem.* 1991; 110:559–565.
16. Coutelle C, Ward PJ, Fleury B, et al. Laryngeal and oropharyngeal cancer and alcohol dehydrogenase 3 and glutathione S-transferase M1 polymorphisms. *Hum Genet.* 1997;99: 319–325.
17. Harty LC, Caporaso NE, Hayes RB, et al. Alcohol dehydrogenase 3 genotype and risk of oral cavity and pharyngeal cancers. *J Natl Cancer Inst.* 1997;89:1698–1705.

18. Yokoyama A, Muramatsu T, Ohmori T, Higuchi S, Hayashida M, Ishii H. Esophageal cancer and aldehyde dehydrogenase-2 genotype in Japanese males. *Cancer Epidemiol Biomarkers Prev.* 1996;5:99–102.
19. Hori H, Kawano T, Endo M, Yuasa Y. Genetic polymorphisms of tobacco- and alcohol-related metabolizing enzymes and human esophageal squamous cell carcinoma susceptibility. *J Clin Gastroenterol.* 1997;25:568–575.
20. Yokoyama A, Muramatsu T, Ohmori T, et al. Alcohol-related cancers and aldehyde dehydrogenase-2 in Japanese alcoholics. *Carcinogenesis.* 1998;19:1383–1387.
21. Nomura T, Noda H, Shibahara T, Yokoyama A, Muramatsu T, Ohmori T. Aldehyde dehydrogenase 2 and glutathione S-transferase M1 polymorphism in relation to the risk for oral cancer in Japanese drinkers. *Oral Oncol.* 2000;36:42–46.
22. Freudenhein JL, Ram M, Nie J, et al. Lung cancer in humans is not associated with lifetime total alcohol consumption or with genetic variation in alcohol dehydrogenase 3 $(ADH_3)^{1,2}$. *J Nutr.* 2003;133:3619–3624.
23. Kato S, Shields PG, Caporaso NE, et al. Cytochrome P450IIE1 genetic polymorphisms, racial variation, and lung cancer risk. *Cancer Res.* 1992;52:6712–6715.
24. El-Zein RA, Zwischenberger JB, Abdel-Rahman SZ, Sankar AB, Au WW. Polymorphism of metabolizing genes and lung cancer histology: prevalence of CYP2E1 in adenocarcinoma. *Cancer Lett.* 1997;112:71–78.
25. Wu X, Shi H, Jiang H, et al. Association between cytochrome P4502E1 genotype, mutagen sensitivity, cigarette smoking and susceptibility to lung cancer. *Carcinogenesis.* 1997;18:967–973.
26. Persson I, Johansson I, Bergling H, et al. Genetic polymorphism of cytochrome P450 2E1 in a Swedish population: relationship to the incidence of lung cancer. *FEBS Lett.* 1993;319:207–211.
27. Marchand LL, Sivaraman L, Pierce L, et al. Association of CYP1A1, GSTM1, and CYP2E1 polymorphisms with lung cancer suggests cell type specificities to tobacco carcinogens. *Cancer Res.* 1998;68:4858–4863.
28. Watanabe J, Yang JP, Eguchi H, et al. An RsaI polymorphism in the CYP2E1 gene does not affect lung cancer risk in a Japanese population. *Jpn J Cancer Res.* 1995;86:245–248.
29. Yamamoto K, Ueno Y, Mizoi Y, Tatsuno Y. Genetic polymorphism of alcohol and aldehyde dehydrogenase and the effects on alcohol metabolism. *Arukoru Kenkyuto Yakubutu Ison.* 1993;28:3–25.
30. Muto M, Nakane M, Hitomi Y, et al. Association between aldehyde dehydrogenase gene polymorphisms and the phenomenon of field cancerization in patients with head and neck cancer. *Carcinogenesis.* 2002;23:1759–1765.
31. Jones AW. Measuring and reporting the concentration of acetaldehyde in human breath. *Alcohol Alcohol.* 1995;30:271–285.
32. Bouchardy C, Hirvonen A, Coutelle C, Ward PJ, Dayer P, Benhamou S. Role of alcohol dehydrogenase 3 and cytochrome P4502E1genotypes in susceptibility to cancers of upper aerodigestive tract. *Int J Cancer.* 2000;87:734–740.
33. Olshan AF, Weissler MC, Watson MA, Bell DA. Risk of head and neck cancer and the alcohol dehydrogenase-3 genotype. *Carcinogenesis.* 2001;22:57–61.
34. Sturgis EM, Dahlstrom KR, Guan Y, et al. Alcohol dehydrogenase 3 genotype is not associated with risk of squamous cell carcinoma of the oral cavity and pharynx. *Cancer Epidemiol Biomarkers Prev.* 2001;10:273–275.
35. Hung HC, Chuang J, Chien YC, et al. Genetic polymorphisms of CYP2E1, GSTM1, and GSTT1; environmental factors and risk of oral cancer. *Cancer Epidemiol Biomarkers Prev.* 1997;6:901–905.
36. Hildesheim A, Anderson LM, Chen CJ, et al. CYP2E1 genetic polymorphisms and risk of nasopharyngeal carcinoma in Taiwan. *J Natl Cancer Inst.* 1997;89:1207–1212.
37. Lin DX, Tang YM, Peng Q, Lu SX, Ambrosone CB, Kadlubar FF. Susceptibility to esophageal cancer and genetic polymorphisms in glutathione S-transferases T1, P1, and M1 and cytochrome P4502E1. *Cancer Epidemiol Biomarkers Prev.* 1998;7:1013–1018.
38. Katoh T, Kaneko S, Kohshi K, et al. Genetic polymorphisms of tobacco- and alcohol-related metabolizing enzymes and oral cavity cancer. *Int J Cancer.* 1999;83:606–609.
39. Watanabe J, Hayashi S, Kawajiri K. Different regulation and expression of the human CYP2E1 gene due to the RsaI polymorphism in the 5′-flanling region. *J Biochem.* 1994;116:321–326.
40. Carriere V, Berthou F, Baird S, Belloe C, Beaune P, de Waziers I. Human cytochrome P450 2E1 (CYP2E1): from genotype to phenotype. *Pharmacogenetics.* 1996;6:203–211.
41. Kim RB, O'Shea D, Wilkinson GR. Intraindividual variability of chlorzoxazone 6-hydroxylation in men and women and its relationship to CYP2E1 genetic polymorphisms. *Clin Phermacol Ther.* 1995;57:645–655.
42. Kim RB, Yamazaki H, Chiba K, et al. In vivo and in vitro characterization of CYP2E1 activity in Japanese and Caucasians. *J Pharmacol Exp Ther.* 1996;279:4–11.

Synergistic antitumor effect of S-1 and the epidermal growth factor receptor inhibitor gefitinib in non-small cell lung cancer cell lines: role of gefitinib-induced down-regulation of thymidylate synthase

Takafumi Okabe,[1] Isamu Okamoto,[1] Sayaka Tsukioka,[3] Junji Uchida,[3] Tsutomu Iwasa,[1] Takeshi Yoshida,[1] Erina Hatashita,[1] Yuki Yamada,[1] Taroh Satoh,[1] Kenji Tamura,[4] Masahiro Fukuoka,[2] and Kazuhiko Nakagawa[1]

[1]Department of Medical Oncology, Kinki University School of Medicine; [2]Department of Internal Medicine, Kinki University School of Medicine, Sakai Hospital, Osaka, Japan; [3]Tokushima Research Center, Taiho Pharmaceutical Co. Ltd., Tokushima, Japan; and [4]Medical Oncology, National Cancer Center Hospital, Tokyo, Japan

Abstract

Somatic mutations in the epidermal growth factor receptor (EGFR) gene are associated with the therapeutic response to EGFR tyrosine kinase inhibitors (TKI) in patients with advanced non-small cell lung cancer (NSCLC). The response rate to these drugs remains low, however, in NSCLC patients with wild-type *EGFR* alleles. Combination therapies with EGFR-TKIs and cytotoxic agents are considered a therapeutic option for patients with NSCLC expressing wild-type *EGFR*. We investigated the antiproliferative effect of the combination of the oral fluorouracil S-1 and the EGFR-TKI gefitinib in NSCLC cells of differing *EGFR* status. The combination of 5-fluorouracil and gefitinib showed a synergistic antiproliferative effect *in vitro* in all NSCLC cell lines tested. Combination chemotherapy with S-1 and gefitinib *in vivo* also had a synergistic antitumor effect on NSCLC xenografts regardless of the absence or presence of *EGFR* mutations. Gefitinib inhibited the expression of the transcription factor E2F-1, resulting in the down-regulation of thymidylate synthase at the mRNA and protein levels. These observations suggest that gefitinib-induced down-regulation of thymidylate synthase is responsible, at least in part, for the synergistic antitumor effect of combined treatment with S-1 and gefitinib and provide a basis for clinical evaluation of combination chemotherapy with S-1 and EGFR-TKIs in patients with solid tumors. [Mol Cancer Ther 2008;7(3):1–8]

Introduction

Targeted therapy in the treatment of cancer has made substantial progress over the last few years. The ErbB family of receptor tyrosine kinases includes the epidermal growth factor receptor (EGFR; ErbB1), ErbB2 (HER2/*neu*), ErbB3, and ErbB4 and is important for normal development as a result of its roles in cell proliferation and differentiation (1–3). Aberrant expression of EGFR has been detected in a wide range of human epithelial malignancies, including non-small cell lung cancer (NSCLC), and is correlated with poor prognosis and reduced survival time (4, 5). Agents that specifically target EGFR are therefore under development as anticancer drugs. Indeed, two inhibitors of the tyrosine kinase activity of EGFR (EGFR-TKI), gefitinib and erlotinib, both of which compete with ATP for binding to the catalytic pocket of the receptor, have been extensively studied in individuals with NSCLC (6–9). Somatic mutations in the region of *EGFR* that encodes the tyrosine kinase domain have been associated with tumor responsiveness to EGFR-TKIs in a subset of NSCLC patients (10–17). In contrast, achievement of a clinical benefit of these drugs in NSCLC patients who express wild-type *EGFR* has been problematic.

S-1 (Taiho Pharmaceutical) is an oral anticancer agent composed of tegafur, 5-chloro-2,4-dihydroxypyridine (CDHP), and potassium oxonate in a molar ratio of 1:0.4:1 (18). Tegafur is a prodrug that generates 5-fluorouracil (5-FU) in blood largely as a result of its metabolism by cytochrome *P*450 in the liver. CDHP increases the plasma concentration of 5-FU through competitive inhibition of dihydropyrimidine dehydrogenase (DPD), which catalyzes 5-FU catabolism (19). Oxonate reduces the gastrointestinal toxicity of 5-FU (20). A response rate of 22% and a median survival time of 10.2 months were obtained in a clinical trial of S-1 in patients with advanced NSCLC not subjected previously to chemotherapy (21). Few severe gastrointestinal or hematologic adverse events were reported. Moreover, a phase II trial of S-1 plus cisplatin in NSCLC patients revealed a 47% response rate and an acceptable safety profile (22).

Based on this background, we examined the anticancer effect of the combination of S-1 and gefitinib in NSCLC cell lines of differing *EGFR* status. We found that the combination of S-1 (or 5-FU) and gefitinib exhibited a marked and synergistic antiproliferative effect both *in vivo*

Received 8/16/07; revised 10/24/07; accepted 1/25/08.

The costs of publication of this article were defrayed in part by the payment of page charges. This article must therefore be hereby marked *advertisement* in accordance with 18 U.S.C. Section 1734 solely to indicate this fact.

Requests for reprints: Isamu Okamoto, Department of Medical Oncology, Kinki University School of Medicine, 377-2 Ohno-higashi, Osaka-Sayama, Osaka 589-8511, Japan. Phone: 81-72-366-0221; Fax: 81-72-360-5000; E-mail: chi-okamoto@dotd.med.kindai.ac.jp.

doi:10.1158/1535-7163.MCT-07-0567

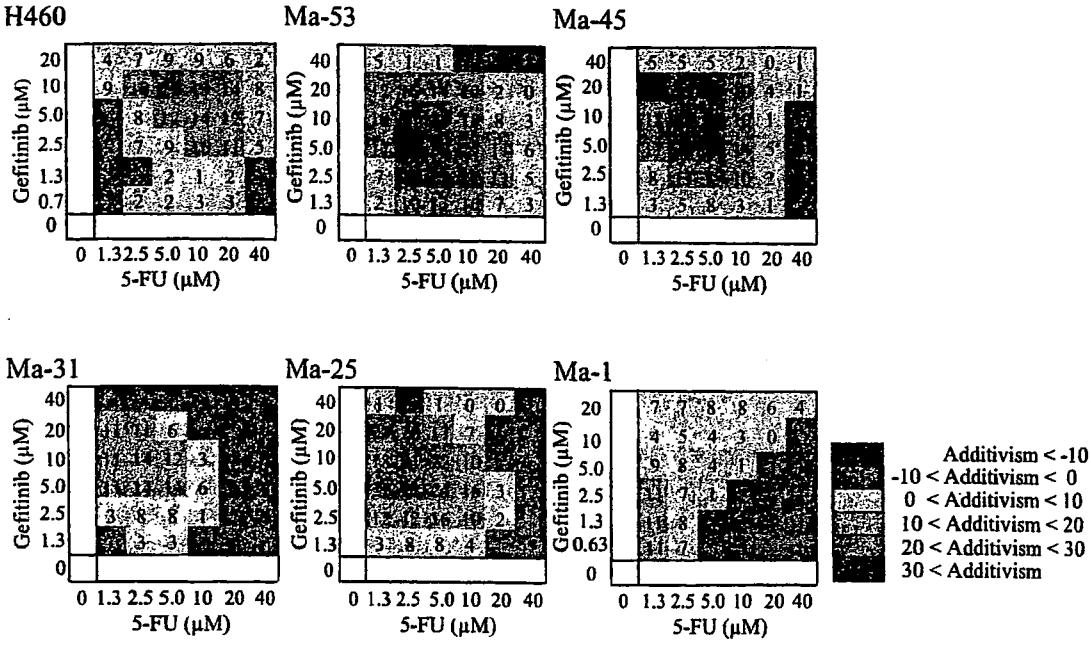

Figure 1. Inhibition of NSCLC cell growth by the combination of 5-FU and gefitinib *in vitro*. Cells with wild-type (H460, Ma-53, Ma-45, Ma-31, and Ma-25) or mutant (Ma-1) EGFR alleles were exposed for 72 h to 5-FU and gefitinib at the indicated concentrations, after which cell viability was measured with a colorimetric assay. The observed excess inhibition (%) relative to that predicted by the Bliss additivism model is shown color-coded in a drug concentration matrix for each cell line. Yellow, orange, pink, and red, synergy; light and dark blue, antagonism. Mean of triplicates from a representative experiment.

and *in vitro* in cells regardless of the absence or presence of *EGFR* mutations. Furthermore, we assessed the effects of gefitinib on the expression of enzymes that function in 5-FU metabolism, including thymidylate synthase (TS), DPD, and orotate phosphoribosyltransferase (OPRT), to gain insight into the mechanism underlying the synergistic effect of combination therapy with S-1 and gefitinib.

Materials and Methods

Cell Lines and Reagents

The human NSCLC cell lines NCI-H460 (H460), Ma-1, Ma-25, Ma-31, Ma-45, and Ma-53 were obtained as described previously (23). MiaPaca-2 cells were obtained from Japan Health Sciences Foundation. These cell lines were cultured under a humidified atmosphere of 5% CO_2 at 37°C in RPMI 1640 (Sigma) supplemented with 10% fetal bovine serum. Gefitinib was provided by AstraZeneca. S-1 and CDHP were provided by Taiho Pharmaceutical. 5-FU was obtained from Wako.

Growth Inhibition Assay *In vitro*

Cells (2.0×10^3) were plated in 96-well flat-bottomed plates and cultured for 24 h before the addition of various concentrations of 5-FU and gefitinib and incubation for an additional 72 h. Cell Counting Kit-8 solution (Dojindo) was then added to each well, and the cells were incubated for 3 h at 37°C before measurement of absorbance at 450 nm. Absorbance values were expressed as a percentage of that for untreated cells, and the concentration of 5-FU or gefitinib resulting in 50% growth inhibition (IC_{50}) was calculated. The effect of combining 5-FU and gefitinib was classified as additive, synergistic, or antagonistic with the Bliss additivism model (24–26). A theoretical curve was calculated for combined inhibition with the equation: $E_{bliss} = E_A + E_B - (E_A \times E_B)$, where E_A and E_B are the fractional inhibitory effects of drug A alone and drug B alone at specific concentrations. E_{bliss} is then the fractional inhibition that would be expected if the effect of the combination of the two drugs was exactly additive. In this study, the Bliss variable is expressed as percentage decrease in cell growth above what would be expected for the combination. Bliss = 0 indicates that the effect of the combination is additive; Bliss > 0 is indicative of synergy; and Bliss < 0 indicates antagonism.

Animals

Male athymic nude mice were exposed to a 12-h light, 12-h dark cycle and provided with food and water *ad libitum* in a barrier facility. All experiments were done in compliance with the regulations of the Animal Experimentation Committee of Taiho Pharmaceutical.

Growth Inhibition Assay *In vivo*

Cubic fragments of tumor tissue (~2 × 2 × 2 mm) were implanted s.c. into the axilla of 5- to 6-week-old male athymic nude mice. Treatment was initiated when tumors in each group achieved an average volume of 100 to 150 mm^3. Treatment groups consisted of control, S-1 alone, gefitinib alone, and the combination of S-1 and gefitinib. Each treatment group contained seven mice. S-1 (10 mg/kg body mass) and gefitinib (50 or 3 mg/kg) were administered by oral gavage once a day for 14 days; control animals

received 0.5% (w/v) hydroxypropylmethylcellulose as vehicle. Tumor volume was determined from caliper measurements of tumor length (*L*) and width (*W*) according to the formula LW^2 / 2. Both tumor size and body weight were measured two or three times per week.

Immunoblot Analysis

Cell lysates were fractionated by SDS-PAGE on 12% gels (NuPAGE Bis-Tris Gels; Invitrogen), and the separated proteins were transferred to a nitrocellulose membrane. After blocking of nonspecific sites with 5% skim milk, the membrane was incubated overnight at room temperature with primary antibodies. Antibodies to DPD, OPRT, and TS were obtained from Taiho Pharmaceutical; those to E2F-1 were from Santa Cruz Biotechnology; and those to β-actin (loading control) were from Sigma. Immune complexes were detected by incubation of the membrane for 1 h at room temperature with horseradish peroxidase–conjugated goat antibodies to mouse or rabbit immunoglobulin and by subsequent exposure to enhanced chemiluminescence reagents (Pierce).

Immunoprecipitation Analysis

Immunoprecipitation of EGFR was done according to standard procedures. Whole-cell lysates (800 μg protein) were incubated overnight at 4°C with antibodies to EGFR (Santa Cruz Biotechnology), after which Protein G Plus/Protein A-Agarose Suspension (Calbiochem) was added and the mixtures were incubated for an additional 1 h at 4°C. Immunoprecipitates were isolated, washed, resolved by SDS-PAGE on a 7.5% gel (Bio-Rad), and subjected to immunoblot analysis with antibodies to phosphotyrosine (PY20) and EGFR (Zymed).

Reverse Transcription and Real-time PCR Analysis

Total RNA (1 μg) extracted from cells with the use of an RNeasy Mini Kit (Qiagen) was subjected to reverse transcription with the use of a SuperScript Preamplification System (Invitrogen Life Technologies). The resulting cDNA was then subjected to real-time PCR analysis with the use of a TaqMan PCR Reagent Kit and a Gene Amp 5700 Sequence Detection System (Applied Biosystems). The forward and reverse primers and TaqMan probe for TS cDNA were 5-GCCTCGGTGTGCCTTTCA-3 and 5-CCCGTGATGTGCGCAAT-3 and 6-FAM-5′-TCGCCAGC-TACGCCCTGCTCA-3′-TAMRA, respectively. Glyceraldehyde-3-phosphate dehydrogenase mRNA were used as an internal standard.

Statistical Analysis

Data are presented as mean ± SE and were analyzed by the Aspin-Welch *t* test. $P < 0.05$ was considered statistically significant.

Results

Effect of the Combination of 5-FU and Gefitinib on NSCLC Cell Growth *In vitro*

Tegafur, which is a component of S-1, is metabolized to 5-FU in the liver and exerts antitumor effects. We first examined the antiproliferative activity of the combination of 5-FU and gefitinib in six NSCLC cell lines. Five of the cell lines (H460, Ma-53, Ma-45, Ma-31, and Ma-25) possess wild-type *EGFR* alleles, whereas Ma-1 cells harbor an EGFR mutation (E746_A750del) that is associated with a high response rate to the EGFR-TKIs gefitinib and erlotinib in individuals with advanced NSCLC. We assessed

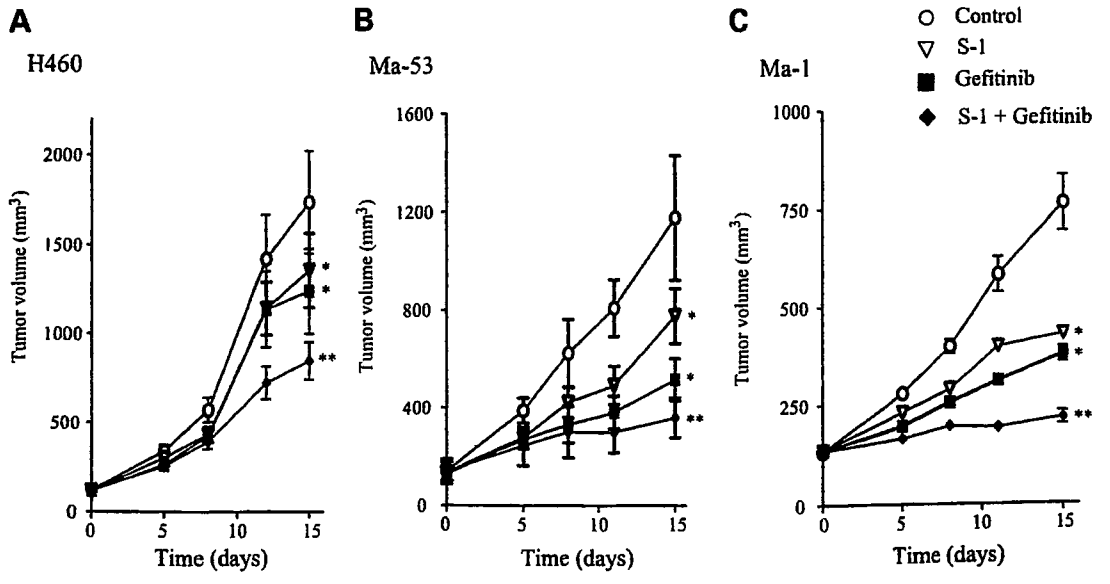

Figure 2. Antitumor activity of the combination of S-1 and gefitinib *in vivo*. **A** and **B**, nude mice with tumor xenografts established by s.c. implantation of NSCLC cells (H460 and Ma-53) possessing wild-type EGFR were treated daily for 2 wk with vehicle (control), S-1 (10 mg/kg), gefitinib (50 mg/kg), or both drugs by oral gavage. **C**, nude mice with tumor xenografts derived from NSCLC cells (Ma-1) expressing mutant EGFR were treated daily for 2 weeks with vehicle (control), S-1 (10 mg/kg), gefitinib (3 mg/kg), or both drugs by oral gavage. Tumor volume in all animals was determined at the indicated times after the onset of treatment. Mean ± SE of values from seven mice per group. *, $P < 0.05$ versus control; **, $P < 0.05$ versus S-1 or gefitinib alone for values 15 d after treatment onset (Aspin-Welch *t* test).

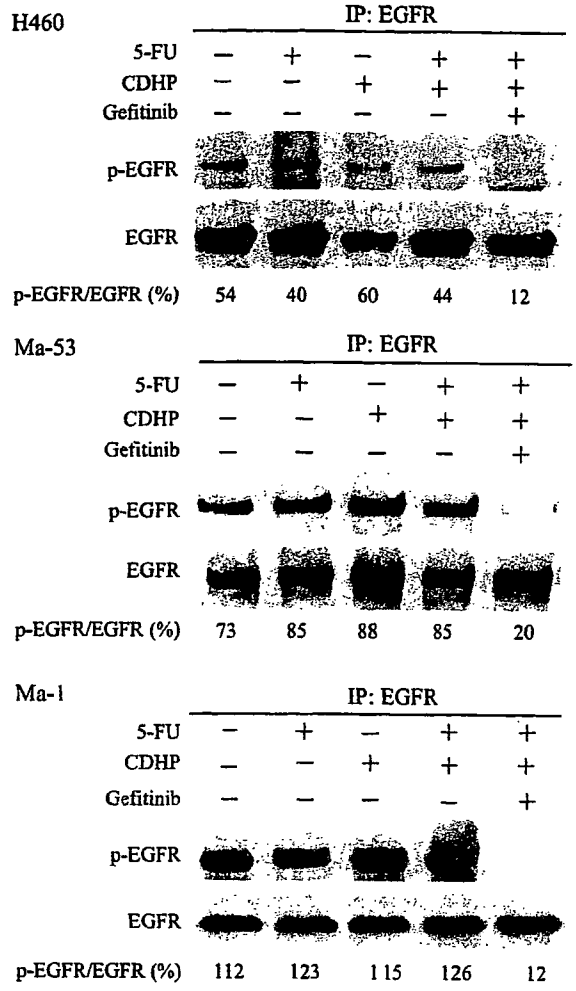

Figure 3. Lack of effect of 5-FU and CDHP on EGFR phosphorylation in NSCLC cell lines. NSCLC cells (H460, Ma-53, and Ma-1) were incubated for 24 h in medium supplemented with 2% fetal bovine serum and with 5-FU (10 μmol/L), CDHP (3 μmol/L), or gefitinib (5 μmol/L). Cell lysates were then prepared and subjected to immunoprecipitation (*IP*) with antibodies to EGFR, and the resulting precipitates were subjected to immunoblot analysis with antibodies to phosphotyrosine (for detection of phosphorylated EGFR) and with antibodies to EGFR. The intensity of the phosphorylated EGFR band relative to that of the EGFR band was determined by densitometry and is expressed as a percentage below each lane.

whether 5-FU and gefitinib showed additivity, synergy, or antagonism based on the Bliss additivism model (24–26). We chose this model rather than isobologram or combination index analysis because it would allow us to evaluate the nature of drug interactions even in instances in which the maximal inhibition by 5-FU or gefitinib alone was too low to obtain a reliable IC_{50} value. The six test concentrations for each agent were chosen after first determining the corresponding IC_{50} values. The IC_{50} values for 5-FU chemosensitivity were not associated with *EGFR* status and ranged from 7 to 11 μmol/L. The effect of combined treatment with 5-FU and gefitinib on the proliferation of the six NSCLC cell lines was tested in triplicate in a 6 × 6 concentration matrix. Calculation of the percentage inhibition in excess of that predicted by the Bliss additivism model revealed synergistic effects of Bliss > 0 for 5-FU and gefitinib in all of the six cell lines tested (Fig. 1). These results suggested that 5-FU and gefitinib act synergistically to inhibit cell growth in NSCLC cells.

Effect of Combined Treatment with S-1 and Gefitinib on NSCLC Cell Growth *In vivo*

We therefore next investigated whether combined treatment with S-1 and gefitinib might also exert a synergistic effect on NSCLC cell growth *in vivo*. Doses of both agents were selected so that their independent effects on tumor growth would be moderate. Nude mice were implanted s.c. with H460, Ma-53, or Ma-1 tumor fragments to establish tumor xenografts. When the H460 or Ma-53 tumors, which harbor wild-type *EGFR*, became palpable (100-150 mm^3), the mice were divided into four groups for daily treatment with vehicle, S-1 (10 mg/kg), gefitinib (50 mg/kg), or both drugs by oral gavage over 2 weeks. For xenografts formed by H460 or Ma-53 cells, combination therapy with S-1 and gefitinib resulted in a significant reduction in tumor size compared with that apparent in animals treated with S-1 or gefitinib alone (Fig. 2*A* and *B*). Mice bearing Ma-1 tumors, which express mutant EGFR, were treated with vehicle, S-1 (10 mg/kg), gefitinib (3 mg/kg), or both agents daily over 2 weeks. Combination treatment with S-1 and gefitinib significantly inhibited the growth of Ma-1 xenografts relative to that apparent in mice treated with either agent alone (Fig. 2C). None of the drug treatments induced a weight loss of >20% during the 2-week period, and no signs of overt drug toxicity were apparent (data not shown). These results thus suggested that combination chemotherapy with S-1 and gefitinib *in vivo* had a synergistic antitumor effect on NSCLC xenografts regardless of the absence or presence of *EGFR* mutations, consistent with our results *in vitro*.

Effects of 5-FU and CDHP on EGFR Phosphorylation in NSCLC Cell Lines

To investigate the mechanism responsible for the observed interaction between S-1 and gefitinib, we examined the effect of 5-FU on EGFR signal transduction in NSCLC cells expressing wild-type (H460 and Ma-53) or mutant (Ma-1) *EGFR*. Immunoprecipitation analysis revealed that exposure of H460 or Ma-53 cells to 5-FU (10 μmol/L) for 24 h had no effect on the basal level of EGFR phosphorylation (Fig. 3). We have shown previously that EGFR is constitutively phosphorylated in Ma-1 cells maintained in serum-free medium (23). Exposure of Ma-1 cells to 5-FU for 24 h did not affect this constitutive level of EGFR phosphorylation (Fig. 3). We next examined the effects of both CDHP, which is a component of S-1, and the combination of CDHP and 5-FU on EGFR phosphorylation in H460, Ma-53, and Ma-1 cells. Neither CDHP alone nor the combination of CDHP and 5-FU affected the level of EGFR phosphorylation in any of these three cell lines (Fig. 3). These results thus indicated that 5-FU and CDHP have no effect on EGFR signal transduction.

Effects of Gefitinib on the Expression of DPD, OPRT, and TS in NSCLC Cell Lines

We next investigated whether gefitinib might affect the expression of DPD, OPRT, or TS, enzymes that are major determinants of the sensitivity of cells to 5-FU. We first examined the abundance of these enzymes in the NSCLC cell lines H460, Ma-53, and Ma-1 by immunoblot analysis. The expression of DPD was detected in MiaPaca-2 cells (positive control) but not in H460, Ma-53, or Ma-1 cells (Fig. 4*A*). In contrast, OPRT and TS were detected in all three NSCLC cell lines and their abundance did not appear related to *EGFR* status (Fig. 4*A*). Treatment of H460, Ma-53, or Ma-1 cells with gefitinib (5 μmol/L) for up to 48 h resulted in a time-dependent decrease in the amount of TS, whereas that of OPRT or DPD remained unaffected (Fig. 4*B*). A reduced level of TS expression in tumors has been associated previously with a higher response rate to 5-FU-based chemotherapy (27, 28). Our data thus suggested that the suppression of TS expression by gefitinib might increase the sensitivity of NSCLC cells to 5-FU.

The transcription factor E2F-1 regulates expression of the TS gene (29–31). We therefore examined the possible effect of gefitinib on E2F-1 expression in NSCLC cell lines. Incubation of H460, Ma-53, or Ma-1 cells with gefitinib for up to 48 h also induced a time-dependent decrease in the amount of E2F-1 (Fig. 4*B*), suggesting that this effect might contribute to the down-regulation of TS expression by gefitinib in these cell lines.

Effect of Gefitinib on TS mRNA Abundance in NSCLC Cell Lines

The abundance of TS mRNA would be expected to be decreased if the down-regulation of E2F-1 expression by gefitinib was responsible for the reduced level of TS. We determined the amount of TS mRNA in H460, Ma-53, or Ma-1 cells at various times after exposure to gefitinib with the use of reverse transcription and real-time PCR analysis. Gefitinib indeed induced a time-dependent decrease in the amount of TS mRNA in all three NSCLC cell lines (Fig. 5), suggesting that the down-regulation of TS expression by gefitinib occurs at the transcriptional level and may be due to suppression of E2F-1 expression.

Discussion

The recent identification of activating somatic mutations of *EGFR* in NSCLC and their relevance to prediction of the therapeutic response to EGFR-TKIs such as gefitinib and erlotinib have had a major effect on NSCLC treatment (10–17). The response rate to these drugs remains low, however, in NSCLC patients with wild-tye *EGFR* alleles. Combination therapy with EGFR-TKIs and cytotoxic agents is a potential alternative strategy for NSCLC expressing wild-type *EGFR*. In the present study, we have evaluated the potential cooperative antiproliferative effect of combined treatment with the EGFR-TKI gefitinib and the new oral fluorouracil S-1 in NSCLC cell lines of differing *EGFR* status. We found that S-1 (or 5-FU) and gefitinib exert a synergistic antiproliferative effect on NSCLC cells both *in vivo* and *in vitro* regardless of the absence or presence of *EGFR* mutation. We chose a gefitinib dose of 50 mg/kg for treatment of mice bearing H460 or Ma-53 tumors. The median effective dose of gefitinib was shown previously to be ~50 mg/kg in athymic nude mice bearing A431 cell-derived xenografts (32). A gefitinib dose of 50 mg/kg has therefore subsequently been widely used in tumor xenograft studies (33–36). The U.S. Food and Drug Administration recommends that drug doses in animals be converted to those in humans based on body surface area (37). According to this guideline, a gefitinib dose of 50 mg/kg in mouse xenograft models is approximately equivalent to the therapeutic dose (250 mg/d) of the drug in humans. In addition, the tumor concentrations of gefitinib in NSCLC xenografts of mice treated with this drug (50 mg/kg) ranged from 9.7 to 13.3 μg/g, values that were similar to the

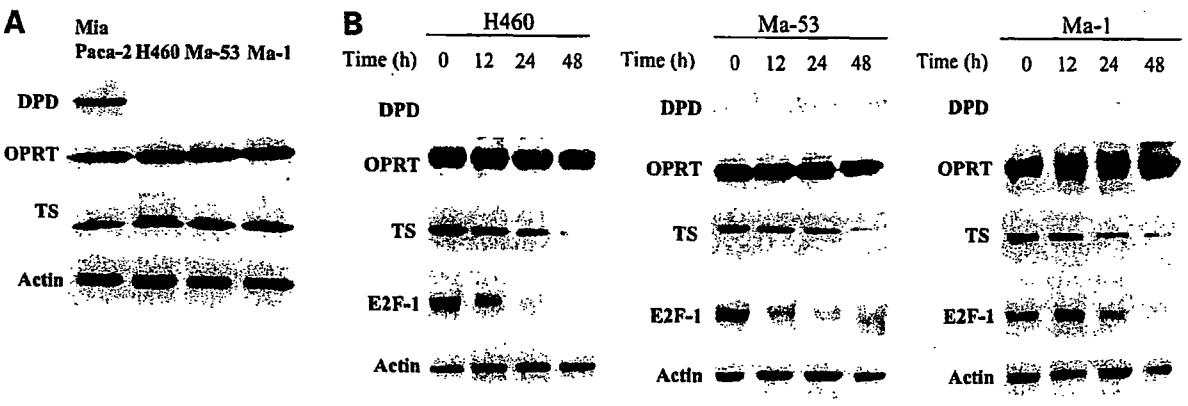

Figure 4. Effects of gefitinib on the expression of E2F-1, DPD, OPRT, and TS in NSCLC cell lines. **A**, lysates of H460, Ma-53, or Ma-1 cells were subjected to immunoblot analysis with antibodies to DPD, OPRT, TS, or β-actin (loading control). MiaPaca-2 cells were also examined as a positive control for DPD expression. **B**, NSCLC cells were incubated with gefitinib (5 μmol/L) for the indicated times in medium containing 10% serum, after which cell lysates were subjected to immunoblot analysis as in **A**, with the addition that E2F-1 expression was also examined.

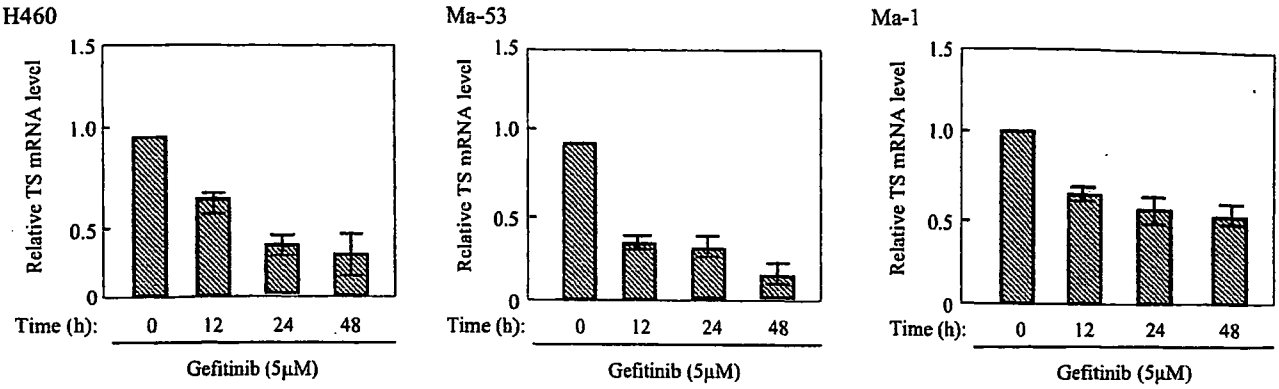

Figure 5. Down-regulation of TS mRNA by gefitinib in NSCLC cell lines. H460, Ma-53, or Ma-1 cells were incubated with gefitinib (5 μmol/L) for the indicated times in medium containing 10% serum, after which total RNA was extracted from the cells and subjected to reverse transcription and real-time PCR analysis of TS mRNA. The amount of TS mRNA was normalized by that of glyceraldehyde-3-phosphate dehydrogenase mRNA. Mean ± SE of values from three separate experiments.

achievable concentrations of gefitinib in tumor tissues of treated humans (34). These observations suggest that a gefitinib dose of 50 mg/kg in mouse xenograft models is appropriate for mimicking the therapeutic dose in humans.

EGFR-TKIs have been shown previously to act synergistically with radiation or cytotoxic agents such as cisplatin, paclitaxel, and irinotecan (38–40). These cytotoxic agents and radiation have been shown to increase the phosphorylation level of EGFR, possibly reflecting the activation of prosurvival signaling, and this effect is blocked by EGFR-TKIs, resulting in the synergistic antitumor effects of the combination therapies. Such a synergistic effect of 5-FU and gefitinib was attributed to 5-FU-induced EGFR phosphorylation in colorectal cancer cells (41). In contrast, we found that 5-FU had no effect on the level of EGFR phosphorylation in NSCLC cell lines. Further examination of different concentrations of 5-FU and different exposure times also failed to reveal an effect of 5-FU on EGFR phosphorylation in these cells (data not shown). These findings indicate that NSCLC cell lines respond differently to 5-FU than do colorectal cancer cells and that the synergistic antiproliferative effect of 5-FU and gefitinib in NSCLC cells is not mediated at the level of EGFR phosphorylation.

Our results indicate that the synergistic interaction of 5-FU (or S-1) and gefitinib is attributable, at least in part, to down-regulation of TS expression by gefitinib. The active metabolite of 5-FU, FdUMP, forms a covalent ternary complex with 5,10-methylenetetrahydrofolate and TS, resulting in inhibition of DNA synthesis (42). TS is thus an important therapeutic target of 5-FU. The amount of TS in neoplastic cells has been found to increase after exposure to 5-FU, resulting in the maintenance of free enzyme in excess of that bound to 5-FU (43–47). Such an increase in TS expression and activity has been viewed as a mechanistic driver of 5-FU resistance in cancer cells (48–50). The development of a new therapeutic strategy that reduces TS expression would therefore be of interest. Indeed, preclinical studies have shown that the down-regulation of TS by antisense oligonucleotides or other means enhances the efficacy of 5-FU (51–54). Down-regulation of TS would be expected to enhance the cytotoxicity of 5-FU as a result of the decrease in the amount of its protein target (55). Consistent with these preclinical data, an inverse relation between TS expression and 5-FU sensitivity has been shown in various human solid tumors (27, 28, 56–60). We have now shown that gefitinib alone induced down-regulation of TS expression, suggesting that this effect of gefitinib contributes to its synergistic interaction with 5-FU (or S-1) in NSCLC cell lines.

We further explored the molecular mechanism by which gefitinib induces down-regulation of TS expression in NSCLC cells. Given that EGFR signal transduction has been shown to be involved in activity of E2F-1 that regulates the expression of several genes including TS (61, 62), which controls the expression of several genes including that for TS, we examined the possible effects of gefitinib on E2F-1 expression and on the abundance of TS mRNA. Gefitinib induced down-regulation of E2F-1 in NSCLC cell lines harboring wild-type *EGFR*, consistent with previous observations (63), as well as in those expressing mutant EGFR. In addition, gefitinib reduced the amount of TS mRNA in NSCLC cells, consistent with the notion that the suppression of TS expression by gefitinib is attributable to inhibition of gene transcription as a result of down-regulation of E2F-1. For our experiments examining the effects of gefitinib on TS and E2F-1 expression, we used a drug concentration of 5 μmol/L. The concentration of gefitinib in tumor xenografts was shown previously to be 5 to 14 times that in the plasma concentration of the mouse hosts (34). Daily oral administration of gefitinib (250 mg) in patients also gave rise to a drug concentration in tumor tissue that was substantially higher (mean, 42-fold) than that in plasma concentration (34). We showed previously that the maximal concentration of gefitinib in the plasma of patients with advanced solid tumors had a mean value of 0.76 μmol/L at a daily dose of 225 mg (64). Based on these data, we considered that a gefitinib concentration of 5 μmol/L was appropriate for our

analyses of TS and E2F-1 expression. Together, our present findings suggest that down-regulation of E2F-1 and consequently that of TS by gefitinib is responsible, at least in part, for the synergistic antitumor effect of combined treatment with S-1 and gefitinib.

Somatic mutations of *EGFR* have been associated with sensitivity to EGFR-TKIs in patients with advanced NSCLC (13–16). However, although most NSCLCs with *EGFR* mutations initially respond to EGFR-TKIs, the vast majority of these tumors ultimately develop resistance to the drug. In the present study, the synergistic effect of combination chemotherapy with S-1 and gefitinib was observed even in *EGFR* mutant cells. Our findings thus suggest that the addition of S-1 (or 5-FU) to EGFR-TKIs might overcome chemoresistance to EGFR-TKIs and that exploration of the effect of such combination therapy in cells resistant to EGFR-TKIs is warranted. *EGFR* mutations appear to be largely limited to lung cancer, with few such mutations having been detected in other types of cancer (65–67). 5-FU is widely used as an anticancer agent and is considered a key drug in chemotherapy for solid tumors such as gastrointestinal and cervical cancer (68–70). Our present results show that gefitinib suppressed the expression of TS in NSCLC cell lines regardless of the absence or presence of *EGFR* mutations, suggesting that the addition of EGFR-TKIs to a 5-FU-containing regimen might increase the effectiveness of such treatment for solid cancers without *EGFR* mutations. Oral combined chemotherapy with drugs, such as S-1 and gefitinib, may also prove to be of low toxicity and therefore maintain quality of life. Our preclinical results provide a basis for future clinical investigations of combination chemotherapy with S-1 and EGFR-TKIs in patients with solid tumors.

References

1. Mendelsohn J, Baselga J. The EGF receptor family as targets for cancer therapy. Oncogene 2000;19:6550–65.
2. Schlessinger J. Cell signaling by receptor tyrosine kinases. Cell 2000; 103:211–25.
3. Hynes NE, Lane HA. ERBB receptors and cancer: the complexity of targeted inhibitors. Nat Rev Cancer 2005;5:341–54.
4. Hirsch FR, Varella-Garcia M, Bunn PA, Jr., et al. Epidermal growth factor receptor in non-small-cell lung carcinomas: correlation between gene copy number and protein expression and impact on prognosis. J Clin Oncol 2003;21:3798–807.
5. Suzuki S, Dobashi Y, Sakurai H, Nishikawa K, Hanawa M, Ooi A. Protein overexpression and gene amplification of epidermal growth factor receptor in nonsmall cell lung carcinomas. An immunohistochemical and fluorescence *in situ* hybridization study. Cancer 2005;103:1265–73.
6. Fukuoka M, Yano S, Giaccone G, et al. Multi-institutional randomized phase II trial of gefitinib for previously treated patients with advanced non-small-cell lung cancer (The IDEAL 1 Trial) [corrected]. J Clin Oncol 2003; 21:2237–46.
7. Perez-Soler R, Chachoua A, Hammond LA, et al. Determinants of tumor response and survival with erlotinib in patients with non-small-cell lung cancer. J Clin Oncol 2004;22:3238–47.
8. Thatcher N, Chang A, Parikh P, et al. Gefitinib plus best supportive care in previously treated patients with refractory advanced non-small-cell lung cancer: results from a randomised, placebo-controlled, multicentre study (Iressa Survival Evaluation in Lung Cancer). Lancet 2005;366:1527–37.
9. Shepherd FA, Rodrigues Pereira J, Ciuleanu T, et al. Erlotinib in previously treated non-small-cell lung cancer. N Engl J Med 2005;353: 123–32.
10. Lynch TJ, Bell DW, Sordella R, et al. Activating mutations in the epidermal growth factor receptor underlying responsiveness of non-small-cell lung cancer to gefitinib. N Engl J Med 2004;350:2129–39.
11. Paez JG, Janne PA, Lee JC, et al. EGFR mutations in lung cancer: correlation with clinical response to gefitinib therapy. Science 2004;304: 1497–500.
12. Pao W, Miller V, Zakowski M, et al. EGF receptor gene mutations are common in lung cancers from "never smokers" and are associated with sensitivity of tumors to gefitinib and erlotinib. Proc Natl Acad Sci U S A 2004;101:13306–11.
13. Mitsudomi T, Kosaka T, Endoh H, et al. Mutations of the epidermal growth factor receptor gene predict prolonged survival after gefitinib treatment in patients with non-small-cell lung cancer with postoperative recurrence. J Clin Oncol 2005;23:2513–20.
14. Takano T, Ohe Y, Sakamoto H, et al. Epidermal growth factor receptor gene mutations and increased copy numbers predict gefitinib sensitivity in patients with recurrent non-small-cell lung cancer. J Clin Oncol 2005;23: 6829–37.
15. Han SW, Kim TY, Hwang PG, et al. Predictive and prognostic impact of epidermal growth factor receptor mutation in non-small-cell lung cancer patients treated with gefitinib. J Clin Oncol 2005;23: 2493–501.
16. Tsao MS, Sakurada A, Cutz JC, et al. Erlotinib in lung cancer—molecular and clinical predictors of outcome. N Engl J Med 2005;353: 133–44.
17. Tokumo M, Toyooka S, Kiura K, et al. The relationship between epidermal growth factor receptor mutations and clinicopathologic features in non-small cell lung cancers. Clin Cancer Res 2005;11:1167–73.
18. Shirasaka T, Shimamoto Y, Fukushima M. Inhibition by oxonic acid of gastrointestinal toxicity of 5-fluorouracil without loss of its antitumor activity in rats. Cancer Res 1993;53:4004–9.
19. Tatsumi K, Fukushima M, Shirasaka T, Fujii S. Inhibitory effects of pyrimidine, barbituric acid and pyridine derivatives on 5-fluorouracil degradation in rat liver extracts. Jpn J Cancer Res 1987;78:748–55.
20. Shirasaka T, Shimamato Y, Ohshimo H, et al. Development of a novel form of an oral 5-fluorouracil derivative (S-1) directed to the potentiation of the tumor selective cytotoxicity of 5-fluorouracil by two biochemical modulators. Anticancer Drugs 1996;7:548–57.
21. Kawahara M, Furuse K, Segawa Y, et al. Phase II study of S-1, a novel oral fluorouracil, in advanced non-small-cell lung cancer. Br J Cancer 2001;85:939–43.
22. Ichinose Y, Yoshimori K, Sakai H, et al. S-1 plus cisplatin combination chemotherapy in patients with advanced non-small cell lung cancer: a multi-institutional phase II trial. Clin Cancer Res 2004;10:7860–4.
23. Okabe T, Okamoto I, Tamura K, et al. Differential constitutive activation of the epidermal growth factor receptor in non-small cell lung cancer cells bearing EGFR gene mutation and amplification. Cancer Res 2007;67:2046–53.
24. Berenbaum MC. Criteria for analyzing interactions between biologically active agents. Adv Cancer Res 1981;35:269–335.
25. Borisy AA, Elliott PJ, Hurst NW, et al. Systematic discovery of multicomponent therapeutics. Proc Natl Acad Sci U S A 2003;100:7977–82. Epub 2003 Jun 10.
26. Buck E, Eyzaguirre A, Brown E, et al. Rapamycin synergizes with the epidermal growth factor receptor inhibitor erlotinib in non-small-cell lung, pancreatic, colon, and breast tumors. Mol Cancer Ther 2006;5:2676–84.
27. Ichikawa W, Uetake H, Shirota Y, et al. Combination of dihydropyrimidine dehydrogenase and thymidylate synthase gene expressions in primary tumors as predictive parameters for the efficacy of fluoropyrimidine-based chemotherapy for metastatic colorectal cancer. Clin Cancer Res 2003;9:786–91.
28. Salonga D, Danenberg KD, Johnson M, et al. Colorectal tumors responding to 5-fluorouracil have low gene expression levels of dihydropyrimidine dehydrogenase, thymidylate synthase, and thymidine phosphorylase. Clin Cancer Res 2000;6:1322–7.
29. DeGregori J, Kowalik T, Nevins JR. Cellular targets for activation by the E2F1 transcription factor include DNA synthesis- and G_1/S-regulatory genes. Mol Cell Biol 1995;15:4215–24.
30. Dyson N. The regulation of E2F by pRB-family proteins. Genes Dev 1998;12:2245–62.
31. Trimarchi JM, Lees JA. Sibling rivalry in the E2F family. Nat Rev Mol Cell Biol 2002;3:11–20.

32. Wakeling AE, Guy SP, Woodburn JR, et al. ZD1839 (Iressa): an orally active inhibitor of epidermal growth factor signaling with potential for cancer therapy. Cancer Res 2002;62:5749–54.

33. Matar P, Rojo F, Cassia R, et al. Combined epidermal growth factor receptor targeting with the tyrosine kinase inhibitor gefitinib (ZD1839) and the monoclonal antibody cetuximab (IMC-C225): superiority over single-agent receptor targeting. Clin Cancer Res 2004;10:6487–501.

34. McKillop D, Partridge EA, Kemp JV, et al. Tumor penetration of gefitinib (Iressa), an epidermal growth factor receptor tyrosine kinase inhibitor. Mol Cancer Ther 2005;4:641–9.

35. Zhang X, Chen ZG, Choe MS, et al. Tumor growth inhibition by simultaneously blocking epidermal growth factor receptor and cyclo-oxygenase-2 in a xenograft model. Clin Cancer Res 2005;11:6261–9.

36. Haura EB, Zheng Z, Song L, Cantor A, Bepler G. Activated epidermal growth factor receptor-Stat-3 signaling promotes tumor survival *in vivo* in non-small cell lung cancer. Clin Cancer Res 2005;11:8288–94.

37. U S. Department of Health and Human Services, Food and Drug Administration, Center for Drug Evaluation and Research (CDER). Guidance for industry, estimating the maximum safe starting dose in initial clinical trials for therapeutics in adult healthy volunteers; 2005. p. 1–27.

38. Koizumi F, Kanzawa F, Ueda Y, et al. Synergistic interaction between the EGFR tyrosine kinase inhibitor gefitinib ("Iressa") and the DNA topoisomerase I inhibitor CPT-11 (irinotecan) in human colorectal cancer cells. Int J Cancer 2004;108:464–72.

39. Chinnaiyan P, Huang S, Vallabhaneni G, et al. Mechanisms of enhanced radiation response following epidermal growth factor receptor signaling inhibition by erlotinib (Tarceva). Cancer Res 2005;65:3328–35.

40. Van Schaeybroeck S, Kyula J, Kelly DM, et al. Chemotherapy-induced epidermal growth factor receptor activation determines response to combined gefitinib/chemotherapy treatment in non-small cell lung cancer cells. Mol Cancer Ther 2006;5:1154–65.

41. Van Schaeybroeck S, Karaiskou-McCaul A, Kelly D, et al. Epidermal growth factor receptor activity determines response of colorectal cancer cells to gefitinib alone and in combination with chemotherapy. Clin Cancer Res 2005;11:7480–9.

42. Peters GJ, van der Wilt CL, van Triest B, et al. Thymidylate synthase and drug resistance. Eur J Cancer 1995;31A:1299–305.

43. Spears CP, Shahinian AH, Moran RG, Heidelberger C, Corbett TH. *In vivo* kinetics of thymidylate synthetase inhibition of 5-fluorouracil-sensitive and -resistant murine colon adenocarcinomas. Cancer Res 1982;42:450–6.

44. Washtien WL. Increased levels of thymidylate synthetase in cells exposed to 5-fluorouracil. Mol Pharmacol 1984;25:171–7.

45. Spears CP, Gustavsson BG, Berne M, Frosing R, Bernstein L, Hayes AA. Mechanisms of innate resistance to thymidylate synthase inhibition after 5-fluorouracil. Cancer Res 1988;48:5894–900.

46. Swain SM, Lippman ME, Egan EF, Drake JC, Steinberg SM, Allegra CJ. Fluorouracil and high-dose leucovorin in previously treated patients with metastatic breast cancer. J Clin Oncol 1989;7:890–9.

47. Chu E, Zinn S, Boarman D, Allegra CJ. Interaction of γ interferon and 5-fluorouracil in the H630 human colon carcinoma cell line. Cancer Res 1990;50:5834–40.

48. Johnston PG, Drake JC, Trepel J, Allegra CJ. Immunological quantitation of thymidylate synthase using the monoclonal antibody TS 106 in 5-fluorouracil-sensitive and -resistant human cancer cell lines. Cancer Res 1992;52:4306–12.

49. Copur S, Aiba K, Drake JC, Allegra CJ, Chu E. Thymidylate synthase gene amplification in human colon cancer cell lines resistant to 5-fluorouracil. Biochem Pharmacol 1995;49:1419–26.

50. Kawate H, Landis DM, Loeb LA. Distribution of mutations in human thymidylate synthase yielding resistance to 5-fluorodeoxyuridine. J Biol Chem 2002;277:36304–11. Epub 2002 Jul 29.

51. Hsueh CT, Kelsen D, Schwartz GK. UCN-01 suppresses thymidylate synthase gene expression and enhances 5-fluorouracil-induced apoptosis in a sequence-dependent manner. Clin Cancer Res 1998;4:2201–6.

52. Ju J, Kane SE, Lenz HJ, Danenberg KD, Chu E, Danenberg PV. Desensitization and sensitization of cells to fluoropyrimidines with different antisenses directed against thymidylate synthase messenger RNA. Clin Cancer Res 1998;4:2229–36.

53. Lee JH, Park JH, Jung Y, et al. Histone deacetylase inhibitor enhances 5-fluorouracil cytotoxicity by down-regulating thymidylate synthase in human cancer cells. Mol Cancer Ther 2006;5:3085–95.

54. Wada Y, Yoshida K, Suzuki T, et al. Synergistic effects of docetaxel and S-1 by modulating the expression of metabolic enzymes of 5-fluorouracil in human gastric cancer cell lines. Int J Cancer 2006;119:783–91.

55. Ferguson PJ, Collins O, Dean NM, et al. Antisense down-regulation of thymidylate synthase to suppress growth and enhance cytotoxicity of 5-FUdR, 5-FU and Tomudex in HeLa cells. Br J Pharmacol 1999;127:1777–86.

56. Aaronson SA. Growth factors and cancer. Science 1991;254:1146–53.

57. Johnston PG, Lenz HJ, Leichman CG, et al. Thymidylate synthase gene and protein expression correlate and are associated with response to 5-fluorouracil in human colorectal and gastric tumors. Cancer Res 1995;55:1407–12.

58. Leichman CG, Lenz HJ, Leichman L, et al. Quantitation of intratumoral thymidylate synthase expression predicts for disseminated colorectal cancer response and resistance to protracted-infusion fluorouracil and weekly leucovorin. J Clin Oncol 1997;15:3223–9.

59. Pestalozzi BC, Peterson HF, Gelber RD, et al. Prognostic importance of thymidylate synthase expression in early breast cancer. J Clin Oncol 1997;15:1923–31.

60. Johnston PG, Mick R, Recant W, et al. Thymidylate synthase expression and response to neoadjuvant chemotherapy in patients with advanced head and neck cancer. J Natl Cancer Inst 1997;89:308–13.

61. Hanada N, Lo HW, Day CP, Pan Y, Nakajima Y, Hung MC. Co-regulation of B-Myb expression by E2F1 and EGF receptor. Mol Carcinog 2006;45:10–7.

62. Ginsberg D. EGFR signaling inhibits E2F1-induced apoptosis *in vivo*: implications for cancer therapy. Sci STKE 2007;pe4.

63. Suenaga M, Yamaguchi A, Soda H, et al. Antiproliferative effects of gefitinib are associated with suppression of E2F-1 expression and telomerase activity. Anticancer Res 2006;26:3387–91.

64. Nakagawa K, Tamura T, Negoro S, et al. Phase I pharmacokinetic trial of the selective oral epidermal growth factor receptor tyrosine kinase inhibitor gefitinib ("Iressa," ZD1839) in Japanese patients with solid malignant tumors. Ann Oncol 2003;14:922–30.

65. Barber TD, Vogelstein B, Kinzler KW, Velculescu VE. Somatic mutations of EGFR in colorectal cancers and glioblastomas. N Engl J Med 2004;351:2883.

66. Lee JW, Soung YH, Kim SY, et al. Absence of EGFR mutation in the kinase domain in common human cancers besides non-small cell lung cancer. Int J Cancer 2005;113:510–1.

67. Shigematsu H, Gazdar AF. Somatic mutations of epidermal growth factor receptor signaling pathway in lung cancers. Int J Cancer 2006;118:257–62.

68. Herskovic A, Martz K, al-Sarraf M, et al. Combined chemotherapy and radiotherapy compared with radiotherapy alone in patients with cancer of the esophagus. N Engl J Med 1992;326:1593–8.

69. Vanhoefer U, Rougier P, Wilke H, et al. Final results of a randomized phase III trial of sequential high-dose methotrexate, fluorouracil, and doxorubicin versus etoposide, leucovorin, and fluorouracil versus infusional fluorouracil and cisplatin in advanced gastric cancer: a trial of the European Organization for Research and Treatment of Cancer Gastrointestinal Tract Cancer Cooperative Group. J Clin Oncol 2000;18:2648–57.

70. Gibson MK, Li Y, Murphy B, et al. Randomized phase III evaluation of cisplatin plus fluorouracil versus cisplatin plus paclitaxel in advanced head and neck cancer (E1395): an Intergroup Trial of the Eastern Cooperative Oncology Group. J Clin Oncol 2005;23:3562–7.

British Journal of Cancer (2007), 1–8

www.bjcancer.com

Full Paper

The novel microtubule-interfering agent TZT-1027 enhances the anticancer effect of radiation *in vitro* and *in vivo*

Y Akashi[1], I Okamoto*[,1], M Suzuki[2], K Tamura[3], T Iwasa[1], S Hisada[4], T Satoh[1], K Nakagawa[1], K Ono[2] and M Fukuoka[1]

[1]Department of Medical Oncology, Kinki University School of Medicine, 377-2 Ohno-higashi, Osaka-Sayama, Osaka 589-8511, Japan; [2]Radiation Oncology Research Laboratory, Research Reactor Institute, Kyoto University, 2-1010 Asashiro-nishi, Kumatori-cho, Sennan-gun, Osaka 590-0494, Japan; [3]Department of Medical Oncology, Kinki University School of Medicine, Nara Hospital, 1248-1 Otodacho, Ikoma,Nara 630-0293, Japan; [4]Asuka Pharmaceutical Co. Ltd, 1604 Shimosakunobe, Takatu-ku, Kawasaki 213-8522, Japan

TZT-1027 is a novel anticancer agent that inhibits microtubule polymerisation and manifests potent antitumour activity in preclinical models. We have examined the effect of TZT-1027 on cell cycle progression as well as the anticancer activity of this drug both *in vitro* and *in vivo*. With the use of tsFT210 cells, which express a temperature-sensitive mutant of Cdc2, we found that TZT-1027 arrests cell cycle progression in mitosis, the phase of the cell cycle most sensitive to radiation. A clonogenic assay indeed revealed that TZT-1027 increased the sensitivity of H460 cells to γ-radiation, with a dose enhancement factor of 1.2. Furthermore, TZT-1027 increased the radiosensitivity of H460 and A549 cells in nude mice, as revealed by a marked delay in tumour growth and an enhancement factor of 3.0 and 2.2, respectively. TZT-1027 also potentiated the induction of apoptosis in H460 cells by radiation both *in vitro* and *in vivo*. Histological evaluation of H460 tumours revealed that TZT-1027 induced morphological damage to the vascular endothelium followed by extensive central tumour necrosis. Our results thus suggest that TZT-1027 enhances the antitumour effect of ionising radiation, and that this action is attributable in part to potentiation of apoptosis induction and to an antivascular effect. Combined treatment with TZT-1027 and radiation therefore warrants investigation in clinical trials as a potential anticancer strategy.
British Journal of Cancer advance online publication, 1 May 2007; doi:10.1038/sj.bjc.6603769 www.bjcancer.com

Keywords: TZT-1027; radiosensitisation; microtubule; mitotic arrest; apoptosis; antivascular effect

The combination of modalities of cancer treatment offers improvements in the survival of cancer patients compared with individual therapeutic approaches. Such therapeutic benefit has been achieved with combinations of chemo- and radiotherapy in a variety of cancers. The cytotoxicity of most chemotherapeutic agents as well as that of radiation is highly dependent on the phase of the cell cycle. Although various types of anticancer drugs are able to arrest cells at specific cell cycle checkpoints, the ability of antimicrotubule agents to block cell cycle progression in G_2-M phase is the biological basis for combination of these agents with radiation (Pawlik and Keyomarsi, 2004). Microtubule-interfering agents have been shown to increase the radiosensitivity of tumour cells in preclinical and clinical studies (Liebmann *et al*, 1994; Choy *et al*, 1995; Edelstein *et al*, 1996; Vokes *et al*, 1996; Kim *et al*, 2001, 2003; Hofstetter *et al*, 2005; Simoens *et al*, 2006).

TZT-1027 (Soblidotin), a novel microtubule-interfering agent synthesised from dolastatin 10 (Figure 1), exhibits greater antitumour activities and a reduced toxicity compared with its parent compound (Miyazaki *et al*, 1995). TZT-1027 inhibits microtubule assembly by binding to tubulin (Kobayashi *et al*, 1997; Natsume *et al*, 2000). *In vitro*, it inhibits the growth of various human cancer cells at low concentrations (Watanabe *et al*, 2000). *In vivo*, TZT-1027 also manifests a broad spectrum of activity against various murine tumours as well as human tumour xenografts, without inducing a pronounced reduction in body weight (Kobayashi *et al*, 1997; Watanabe *et al*, 2000, 2006a; Natsume *et al*, 2003, 2006). Furthermore, the drug exhibited a potent antivascular effect on existing vasculature in an advanced-stage tumour model (Otani *et al*, 2000). TZT-1027 is currently undergoing clinical evaluation, with a reduction in tumour size and disease stabilisation having been observed in a subset of patients (Schoffski *et al*, 2004; de Jonge *et al*, 2005; Greystoke *et al*, 2006; Tamura *et al*, 2007).

Despite its demonstrated efficacy against solid tumours, the effects of TZT-1027 in combination with radiation have not been examined. As an initial step in determining the antitumour activity of TZT-1027 in combination with radiation, we investigated the effect of this agent on cell cycle progression in synchronised tsFT210 cells (Osada *et al*, 1997), which harbour a temperature-sensitive mutant of Cdc2. We found that TZT-1027 induces arrest of cells in mitosis, the phase of the cell cycle most sensitive to radiation. We then studied the radiosensitising properties of TZT-1027 *in vitro* and *in vivo* with a human lung cancer model and elucidated the mechanism of radiosensitisation by this agent.

*Correspondence: Dr I Okamoto;
E-mail: okamoto@dotd.med.kindai.ac.jp
Revised 28 February 2007; accepted 2 April 2007

MATERIALS AND METHODS

Cell lines and reagents

tsFT210 mouse mammary carcinoma cells, which express a temperature-sensitive mutant of Cdc2, were kindly provided by H Kakeya (Antibiotics Laboratory, Discovery Research Institute, RIKEN, Saitama, Japan) and were maintained under a humidified atmosphere of 5% CO_2 in air at 32.0°C in RPMI 1640 (Sigma, St Louis, MO, USA) supplemented with 10% foetal bovine serum and 1% penicillin-streptomycin. H460 human lung large cell carcinoma and A549 human lung adenocarcinoma cells were obtained from American Type Culture Collection (Manassas, VA, USA) and were maintained as for tsFT210 cells with the exception that the culture temperature was 37°C. TZT-1027 (Figure 1) was provided by Daiichi Pharmaceutical Co. Ltd (Tokyo, Japan). Nocodazole and roscovitine were obtained from Sigma.

Cell cycle analysis

Cells were harvested, washed with phosphate-buffered saline (PBS), fixed with 70% methanol, washed again with PBS, and stained with propidium iodide (0.05 mg ml^{-1}) in a solution containing 0.1% Triton X-100, 0.1 mM EDTA, and RNase A (0.05 mg ml^{-1}). The stained cells ($\sim 1 \times 10^6$) were then analysed for DNA content with a flow cytometer (FACScalibur; Becton Dickinson, San Jose, CA, USA).

Measurement of mitotic index and apoptotic cells

Cells were harvested, washed with PBS, fixed with methanol : acetic acid (3 : 1, v/v), washed again with PBS, and stained with 4′,6-diamidino-2-phenylindole (DAPI) (0.5 μg ml^{-1}). The stained cells ($\sim 1 \times 10^6$) were observed with a fluorescence microscope (IX71; Olympus, Tokyo, Japan). To determine the proportion of mitotic or apoptotic cells, we scored at least 300 cells in each of at least three randomly selected microscopic fields for each of three slides per sample. Cells with condensed chromosomes and no obvious nuclear membrane were regarded as mitotic cells, and the mitotic index was calculated as the percentage of mitotic cells among total viable cells. Cells with fragmented and uniformly condensed nuclei were regarded as apoptotic cells.

Clonogenic assay

Exponentially growing H460 cells in 25-cm^2 flasks were harvested by exposure to trypsin and counted. They were diluted serially to appropriate densities and plated in triplicate in 25-cm^2 flasks containing 10 ml of medium. The cells were treated with 1 nM TZT-1027 or vehicle (dimethyl sulfoxide, or DMSO; final concentration, 0.1%) for 24 h and then exposed to various doses of γ-radiation with a ^{60}Co irradiator at a rate of $\sim$0.82 Gy min^{-1} and at room temperature. The cells were then washed with PBS, cultured in drug-free medium for 10–14 days, fixed with methanol : acetic acid (10 : 1, v/v), and stained with crystal violet. Colonies containing >50 cells were counted. The surviving fraction was calculated as: (mean number of colonies)/(number of inoculated cells × plating efficiency). Plating efficiency was defined as the mean number of colonies divided by the number of inoculated cells for nonirradiated controls. The surviving fraction for combined treatment was corrected by that for TZT-1027 treatment alone. The dose enhancement factor (DEF) was calculated as the dose (Gy) of radiation that yielded a surviving fraction of 0.1 for vehicle-treated cells divided by that for TZT-1027-treated cells (after correction for drug toxicity).

In vivo antitumour activity of TZT-1027 with or without radiation

All animal studies were performed in accordance with the Recommendations for Handling of Laboratory Animals for Biomedical Research, compiled by the Committee on Safety and Ethical Handling Regulations for Laboratory Animal Experiments, Kyoto University. The ethical guidelines followed meet the requirements of the UKCCCR guidelines (Workman *et al*, 1998). Tumour cells (2×10^6) were injected subcutaneously into the right hind leg of 7-week-old female athymic nude mice. Tumour volume was determined from caliper measurement of tumour length (L) and width (W) according to the formula $LW^2/2$. Treatment was initiated when tumours in each group achieved an average volume of $\sim$200–250 mm^3. Treatment groups consisted of control, TZT-1027 alone, radiation alone, and the combination of TZT-1027 and radiation. Each treatment group contained six to eight mice. TZT-1027 was administered intravenously in a single dose of 0.5 mg kg^{-1} of body weight; mice in the control and radiation-alone groups were injected with vehicle (physiological saline). Tumours in the leg were exposed to 10 Gy of γ-radiation with a ^{60}Co irradiator at a rate of $\sim$0.32 Gy min^{-1} immediately after drug treatment. Growth delay (GD) was calculated as the time for treated tumours to achieve an average volume of 500 mm^3 minus the time for control tumours to reach 500 mm^3. The enhancement factor was then determined as: $(GD_{combination} - GD_{TZT-1027})/(GD_{radiation})$.

TUNEL staining

Mice were killed 14 days after treatment initiation and the tumours were removed and preserved in 10% paraformaldehyde. Apoptosis in tumour sections was determined by the terminal deoxynucleotidyl transferase-mediated dUTP-biotin nick-end labelling (TUNEL) assay with the use of an apoptosis detection kit (Chemicon, Temecula, CA, USA). The number of apoptotic cells was counted in 10 separate microscopic fields (× 100) for three sections of each tumour of each group.

Histological analysis

A single dose of TZT-1027 (2.0 mg kg^{-1}) or vehicle (physiological saline) was administered intravenously to mice when H460 tumours had achieved a volume of $\sim$400 to 600 mm^3. Tumour tissue was extirpated 4 or 24 h after drug administration, and half of the tissue was fixed in 10% buffered formalin, embedded in paraffin, sectioned, and stained with hematoxylin-eosin. The other half of the tumour tissue was fixed for 12–48 h in zinc fixative

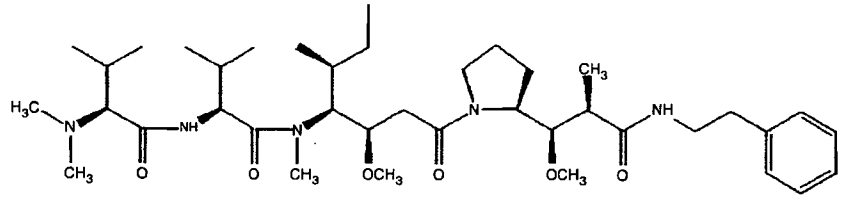

Figure 1 Chemical structure of TZT-1027.

(BD Biosciences, San Jose, CA, USA), embedded in paraffin, sectioned, and immunostained for CD31. Endogenous peroxidase activity was blocked by incubation of the latter sections for 20 min with 0.3% H_2O_2 in methanol, and nonspecific sites were blocked with antibody diluent (Dako Japan, Kyoto, Japan). Sections were then incubated overnight at 4°C with a 1:50 dilution of a rat monoclonal antibody to mouse CD31 (BD Biosciences), washed with PBS, and processed with a Histfine Simple Stain PO (M) kit (Nichirei, Tokyo, Japan) for detection of immune complexes. Sections were counterstained with Mayer's hematoxylin, covered with a coverslip with the use of a permanent mounting medium, and examined with a light microscope (CX41; Olympus, Tokyo, Japan).

Statistical analysis

Data are presented as means ± s.d. or s.e. and were compared by the unpaired Student's *t*-test. A P value of <0.05 was considered statistically significant.

RESULTS

Induction of cell cycle arrest at M phase but not at G_1-S in tsFT210 cells by TZT-1027

To examine the effect of TZT-1027 on cell cycle progression, we performed flow cytometric analysis of tsFT210 cells, which express a temperature-sensitive mutant of Cdc2. These mammary carcinoma cells exhibit a normal cell cycle distribution when incubated at the permissive temperature of 32.0°C, but they arrest at G_2 phase as a result of Cdc2 inactivation when incubated at the nonpermissive temperature of 39.4°C (Figure 2A and B). We synchronised tsFT210 cells at G_2 phase by incubation at 39.4°C for 17 h and then cultured them at 32.0°C for 6 h in the presence of nocodazole (an inhibitor of microtubule polymerisation), TZT-1027, or vehicle (DMSO). In the presence of vehicle alone, the number of cells in G_2 phase decreased markedly and there was a corresponding increase in the number of cells in G_1 phase, indicative of re-entry of cells into the cell cycle (Figure 2C). In contrast, treatment with nocodazole or TZT-1027 prevented the cells from passing through G_2-M phase (Figure 2D and E). Given that flow cytometric analysis did not distinguish between cells in M phase and those in G_2 phase, we determined the mitotic index of cells by DAPI staining and fluorescence microscopy. Most of the cells released from temperature-induced arrest in the presence of nocodazole manifested condensed chromosomes without a nuclear membrane, yielding a mitotic index of 93%; most of the cells had thus arrested in mitosis (Figure 2D). Most of the cells released from temperature-induced arrest in the presence of TZT-1027 showed similar mitotic figures, yielding a mitotic index of 85% (Figure 2E) and demonstrating that TZT-1027 also inhibits cell cycle progression at mitosis.

We next examined whether TZT-1027 affects the G_1-S transition. We arrested tsFT210 cells at G_2 phase by incubation at 39.4°C, released the cells into G_1 phase by shifting to the permissive temperature for 6 h, and then incubated them for an additional 6 h in the presence of roscovitine (an inhibitor of CDK2 that prevents cell cycle progression at G_1 phase), TZT-1027, or vehicle (Figure 3). The cells incubated with vehicle passed through G_1 phase and yielded a broad S-phase peak (Figure 3D), whereas those treated with roscovitine did not pass through G_1 phase (Figure 3E). In contrast, TZT-1027 had no effect on passage of the synchronised tsFT210 cells through the G_1-S transition (Figure 3F). Together,

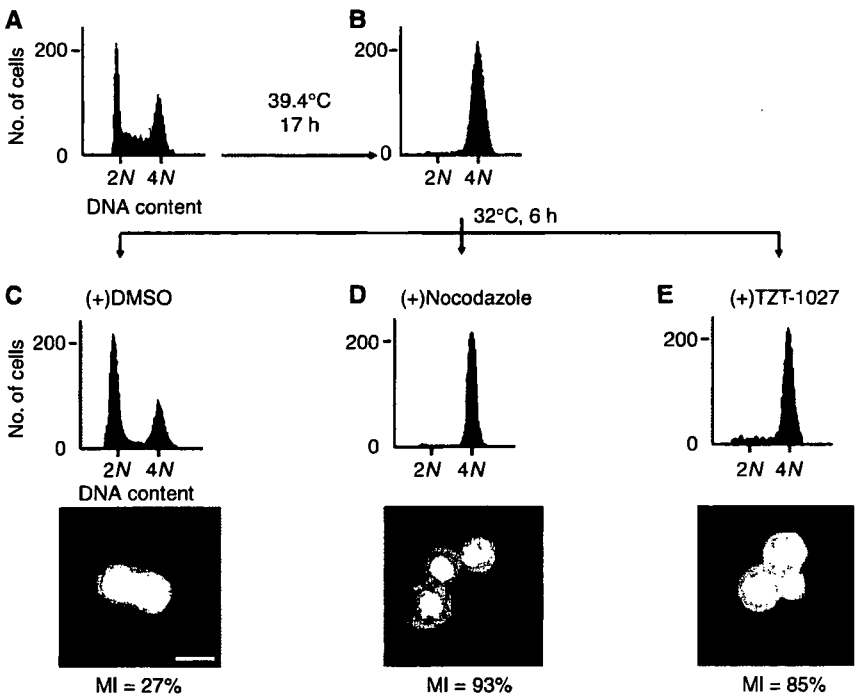

Figure 2 Inhibition of tsFT210 cell cycle progression through G_2-M by TZT-1027. Cells were cultured at the permissive temperature of 32.0°C (**A**) and then incubated for 17 h at the nonpermissive temperature of 39.4°C (**B**). They were subsequently released from G_2 arrest by incubation at 32.0°C for 6 h in the presence of DMSO (**C**), 1 μM nocodazole (**D**), or 2 nM TZT-1027 (**E**). At each stage of the protocol, cells were analysed for DNA content by staining with propidium iodide and flow cytometry. The 2N and 4N peaks indicate cells in G_0-G_1 and G_2-M phases of the cell cycle, respectively. The cells were also stained with DAPI and examined by fluorescence microscopy after treatment with DMSO, nocodazole, or TZT-1027 (lower panels), and the mitotic index (MI) was determined; scale bar, 20 μm. Data are representative of at least three independent experiments.

these results indicate that the effect of TZT-1027 on cell cycle progression is specific to M phase.

Induction of cell cycle arrest at M phase in asynchronous H460 cells by TZT-1027

We next examined whether TZT-1027 induced mitotic arrest in asynchronous H460 human non-small cell lung cancer cells. Flow cytometric analysis revealed that treatment of H460 cells with TZT-1027 for 24 h induced a threefold increase in the proportion of cells with a DNA content of 4N compared with that apparent for vehicle-treated cells (29.1 *vs* 8.7%) (Figure 4A and B). Furthermore, DAPI staining revealed that TZT-1027 induced a significant increase in the mitotic index of H460 cells compared with that for the control cells (23.3 *vs* 4.6%) (Figure 4C and D), indicating that most of the TZT-1027-treated cells with a DNA content of 4N were arrested in M phase rather than in G_2 phase. These observations thus showed that TZT-1027 also induced mitotic arrest in asynchronous H460 cells.

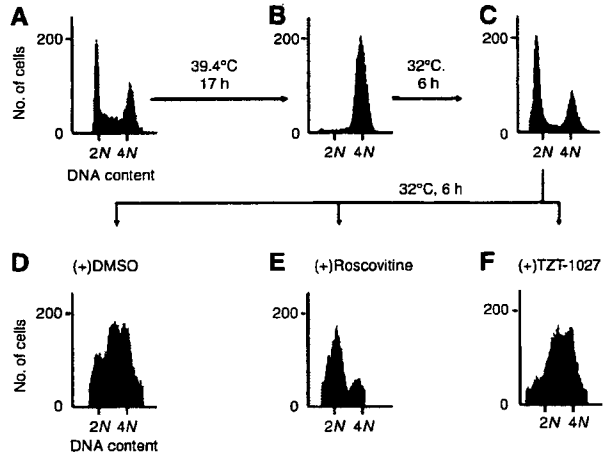

Figure 3 Lack of effect of TZT-1027 on tsFT210 cell cycle progression through G_1-S. Exponentially growing tsFT210 cells (**A**) were arrested in G_2 phase by incubation for 17 h at 39.4°C (**B**). The cells were incubated at 32.0°C first for 6 h to allow progression to G_1 phase (**C**) and then for an additional 6 h in the presence of DMSO (**D**), 50 μM roscovitine (**E**), or 2 nM TZT-1027 (**F**). At each stage of the protocol, cells were analysed for DNA content by flow cytometry. Data are representative of at least three independent experiments.

Radiosensitisation of H460 cells by TZT-1027 *in vitro*

Cells in M phase are more sensitive to radiation than are those in other phases of the cell cycle. Given that exposure of H460 cells to TZT-1027-induced mitotic arrest, we next examined whether this agent might sensitise H460 cells to γ-radiation with the use of a clonogenic assay. H460 cells were incubated for 24 h with 1 nM TZT-1027 or vehicle (DMSO) and then exposed to various doses (0, 2, 4, or 6 Gy) of γ-radiation. The cells were then allowed to form colonies in drug-free medium for 10–14 days. Survival curves revealed that TZT-1027 increased the radiosensitivity of H460 cells, with a DEF of 1.2 (Figure 5A).

To determine whether radiosensitisation by TZT-1027 was reflected by an increase in the proportion of apoptotic cells, we exposed H460 cells to 1 nM TZT-1027 or vehicle for 24 h, treated the cells with various doses (0, 2, 4, or 6 Gy) of radiation, and then incubated them in drug-free medium for an additional 24 h before quantification of apoptosis. Combined treatment with TZT-1027 and 4 or 6 Gy of radiation resulted in a significant increase in the number of apoptotic cells compared with the sum of the values for treatment with drug alone or radiation alone (Figure 5B). TZT-1027 thus promoted radiation-induced apoptosis in H460 cells.

Radiosensitisation of H460 cells and A549 cells by TZT-1027 *in vivo*

To determine whether the TZT-1027-induced increase in the radiosensitivity of tumour cells observed *in vitro* might also be apparent *in vivo*, we injected H460 cells or A549 human lung

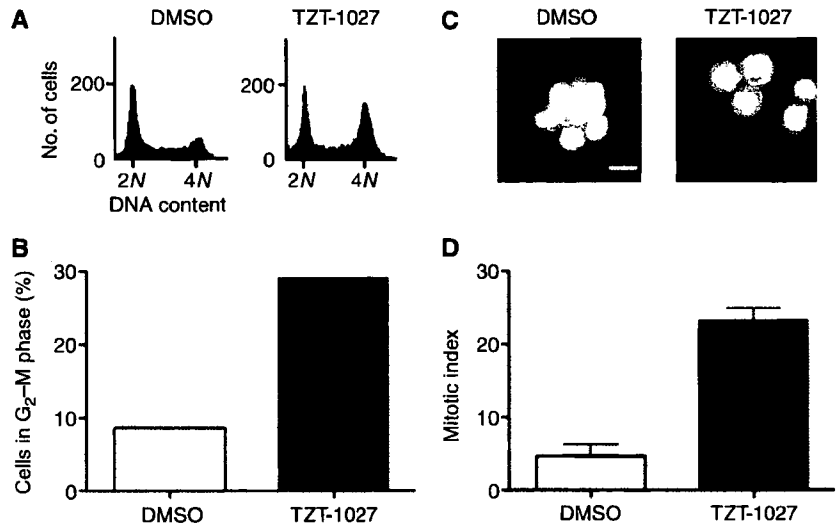

Figure 4 Induction of cell cycle arrest at M phase in H460 cells by TZT-1027. H460 cells were incubated in the presence of 1 nM TZT-1027 or vehicle (DMSO) for 24 h, after which DNA content was measured by flow cytometry (**A**) and the fraction of cells in G_2-M phase was determined (**B**). The cells were also stained with DAPI and examined by fluorescence microscopy (**C**) and the mitotic index was determined (**D**). Data in (**A**) through (**C**) are representative of at least three independent experiments; data in (**D**) are means ± s.d. of values from three independent experiments. Scale bar in (**C**), 20 μm.

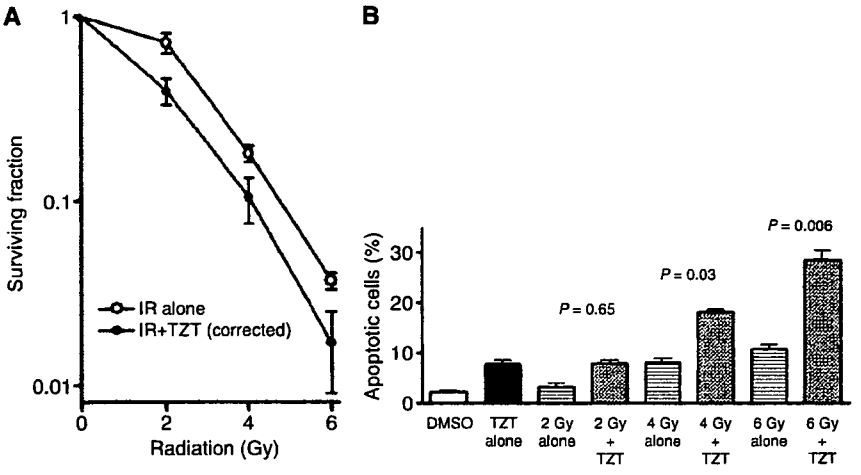

Figure 5 Sensitisation of H460 cells to γ-radiation by TZT-1027 *in vitro*. (**A**) Clonogenic assay. Cells were incubated with 1 nM TZT-1027 or vehicle (DMSO) for 24 h, exposed to the indicated doses of γ-radiation, and then incubated in drug-free medium for 10–14 days for determination of colony-forming ability. Survival curves were generated after correction of colony formation observed for combined treatment with ionising radiation (IR) and TZT-1027 by that apparent for treatment with TZT-1027 alone. (**B**) Assay of apoptosis. Cells were incubated with 1 nM TZT-1027 or vehicle (DMSO) for 24 h, exposed to various doses (0, 2, 4, or 6 Gy) of γ-radiation, and then incubated for 24 h in drug-free medium. Cells were then fixed and stained with DAPI for determination of the proportion of apoptotic cells by fluorescence microscopy. Data in (**A**) and (**B**) are means ± s.d. of values from three independent experiments. *P* values in (**B**) are for comparison of the value for combined treatment with TZT-1027 and radiation *vs* the sum of the corresponding values for each treatment alone, after correction of all data by the control (DMSO) value.

adenocarcinoma cells into nude mice in order to elicit the formation of solid tumours. The mice were then treated with TZT-1027, radiation, or both modalities. Treatment with TZT-1027 alone (single dose of 0.5 mg kg^{-1}) or with radiation alone (single dose of 10 Gy) resulted in relatively small inhibitory effects on tumour growth, whereas combined treatment with both TZT-1027 and radiation exerted a markedly greater inhibitory effect (Figure 6A and B). The tumour GDs induced by treatment with TZT-1027 alone, radiation alone, or both TZT-1027 and radiation were 1.0, 2.6, and 8.8 days, respectively, for H460 cells and 1.4, 4.9, and 12.4 days, respectively, for A549 cells (Table 1). The enhancement factor for the effect of TZT-1027 on the efficacy of radiation was 3.0 for H460 cells and 2.2 for A549 cells, revealing the effect to be greater than additive. No pronounced tissue damage or toxicities such as diarrhoea or weight loss of > 10% were observed in mice in any of the four treatment groups (Table 2).

We examined the effects of the treatment protocols on apoptosis in H460 tumours by TUNEL staining of tumour sections. Quantification of the number of apoptotic cells revealed that the combined treatment with radiation and TZT-1027 induced a significant increase in this parameter compared with treatment with radiation or TZT-1027 alone (Figure 6C).

Histological appearance of H460 tumours after administration of TZT-1027

Finally, we examined whether an effect of TZT-1027 on tumour vasculature might contribute to the antitumour activity of this drug *in vivo*. Mice harbouring H460 tumours were injected with TZT-1027, and the tumours were excised 4 or 24 h thereafter and examined by hematoxylin-eosin staining (Figure 7A–C) or by immunostaining for the endothelial cell marker CD31 (Figure 7D and E). Tumour capillaries appeared congested, with thrombus formation, and showed a loss of endothelial cells 4 h after administration of TZT-1027 (Figure 7B and E), whereas vessels within viable areas of control tumours were generally not congested and showed an intact normal endothelium (Figure 7A and D). The effects of TZT-1027 on the tumour vasculature appeared selective, given that neither loss of CD31 staining nor vessel congestion was apparent in the vasculature of surrounding normal tissue after drug treatment (Figure 7E). Extensive necrosis was apparent at the tumour core, with a characteristic thin rim of viable tumour cells remaining at the periphery, 24 h after TZT-1027 administration (Figure 7C). These results were thus indicative of a characteristic antivascular effect of TZT-1027 in the H460 tumour model.

DISCUSSION

TZT-1027 is a novel antitumour agent that inhibits microtubule polymerisation and exhibits potent antitumour activity in preclinical models (Miyazaki *et al*, 1995; Kobayashi *et al*, 1997; Natsume *et al*, 2000, 2003, 2006; Otani *et al*, 2000; Watanabe *et al*, 2000, 2006a). We investigated the effect of TZT-1027 on cell cycle progression with the use of tsFT210 cells, which can be synchronised in G_2 phase by incubation at 39.4°C and consequent inactivation of Cdc2 (Osada *et al*, 1997; Tamura *et al*, 1999). The use of these cells allows cell synchronisation without the need for agents that prevent DNA synthesis (such as hydroxyurea or thymidine) or that inhibit formation of the mitotic spindle (such as nocodazole). Although such agents halt cell cycle progression in specific phases of the cycle, they are also toxic and kill a proportion of the treated cells. The tsFT210 cell system is thus suited to sensitive analysis of the effects of new compounds on cell cycle progression without loss of cell viability. We have now shown that tsFT210 cells released from G_2 arrest by incubation at 32.0°C failed to pass through M phase in the presence of TZT-1027. Although previous flow cytometric analysis of exponentially growing tumour cells revealed that TZT-1027 induced a marked increase in the proportion of cells in G_2-M (Watanabe *et al*, 2000), it was uncertain whether the drug arrested cell cycle progression in G_2 or in mitosis. Our morphological data now indicate that, similar to the effect of nocodazole, TZT-1027 arrested tsFT210 cells in M phase rather than in G_2, consistent with the mode of action of this new compound. Given that microtubules contribute to various cellular functions in addition to cell division, including intracellular transport and signal transduction (Mollinedo and Gajate,

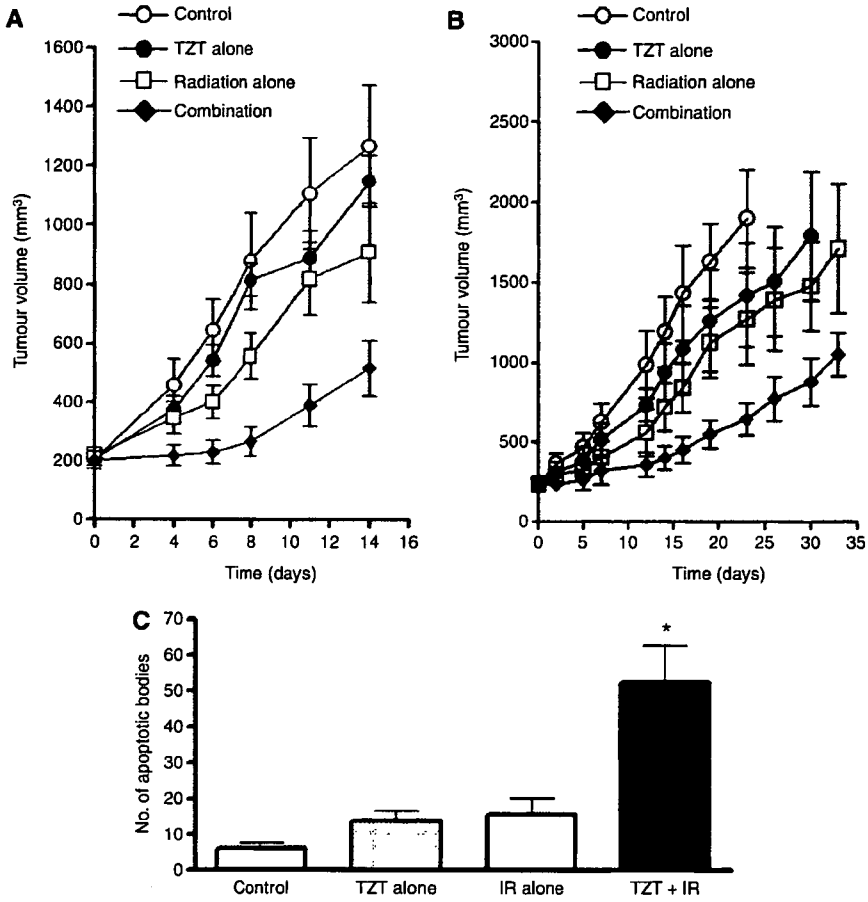

Figure 6 Sensitisation of H460 and A549 cells to γ-radiation by TZT-1027 *in vivo*. (**A** and **B**) Evaluation of tumour growth. Nude mice with H460 (**A**) or A549 (**B**) tumour xenografts (~200 to 250 mm^3) were treated with a single intravenous dose of TZT-1027 (0.5 mg kg^{-1}), a single dose of γ-radiation (10 Gy), or neither (control) or both modalities, and tumour volume was determined at the indicated times thereafter. Data are means ± s.e. for six to eight mice per group. (**C**) Quantification of apoptotic cells in H460 tumour sections by TUNEL staining 14 days after the initiation of treatment as in (**A**). Data are means ± s.d. *$P < 0.05$ *vs* mice treated with TZT-1027 alone or radiation alone.

Table 1 Tumour growth delay value

	H460		A549	
Treatment	**Days[a]**	**GD[b]**	**Days**	**GD**
Control	4.5		5.5	
TZT-1027 alone	5.5	1	6.9	1.4
Radiation alone	7.1	2.6	10.4	4.9
TZT-1027 + Radiation	13.3	8.8	17.9	12.4
Enhancement factor	3		2.2	

[a]Days, the period needed for the sizes of xenografts in each group to reach 500 mm^3; [b]GD, the additional periods needed for the sizes of xenografts in each group to reach 500 mm^3 in addition to the period needed for controls to reach 500 mm^3.

Table 2 Body weight loss

	% of B.W.L[a]	
	H460	**A549**
Control	3.6	1.2
TZT-1027 alone	9.9	5.2
Radiation alone	9.7	5.5
TZT-1027+Radiation	8.7	9.9

[a]% of B.W.L, relative body weight loss 7 days after the initiation of the treatment.

2003), TZT-1027 might also be expected to affect tumour cells in interphase. With the use of synchronised tsFT210 cells, however, we found that TZT-1027 had no effect on progression of cells through the G_1–S transition of the cell cycle. The effect of TZT-1027 on cell cycle progression thus appears to be specific to M phase.

Given that cells are most sensitive to radiation during mitosis (Sinclair and Morton, 1966; Sinclair, 1968; Pawlik and Keyomarsi, 2004), we next investigated the possible interaction between TZT-1027 and ionising radiation in human lung cancer cell lines. We found that TZT-1027 increased the sensitivity of H460 cells to γ-radiation *in vitro*. The proportion of H460 cells in mitotic phase at the time of irradiation was increased by TZT-1027 treatment, consistent with the notion that this effect contributes to the observed radiosensitisation induced by this drug. TZT-1027 was previously shown to induce apoptosis in several tumour cell lines (Watanabe *et al*, 2000). Although the relation between apoptosis and radiosensitivity is controversial (Lawrence *et al*, 2001; Pawlik and Keyomarsi, 2004), we showed that treatment of H460 cells with

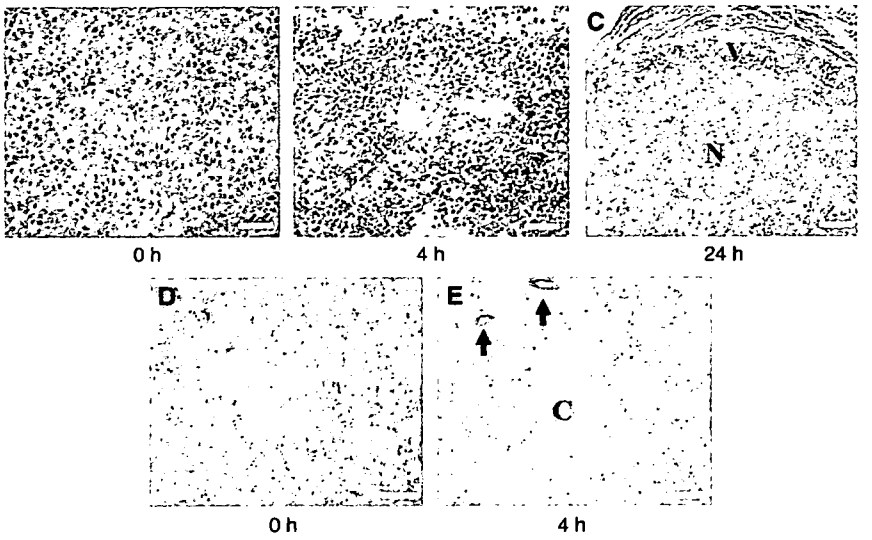

Figure 7 Histological analysis of H460 tumours after treatment with TZT-1027. Mice bearing H460 tumour xenografts were treated with a single dose of TZT-1027 (2.0 mg kg^{-1}), and the tumours were excised at various times thereafter and either stained with hematoxylin-eosin (**A**–**C**) or immunostained for CD31 (**D** and **E**). (**A** and **D**) Control sections of an untreated tumour showing normal capillaries with an intact endothelium and viable tumour cells. (**B** and **E**) Sections of a tumour removed 4 h after administration of TZT-1027. Vascular congestion, with pink deposits of fibrin, and loss of endothelial cells as well as diffuse tumour cell degeneration are apparent in (**b**). Dark immunostaining of intact endothelium (arrows) is apparent in surrounding normal connective tissue, whereas little staining of endothelial cells was observed in the core (**C**) of the tumour (**E**). (**C**) Section of a tumour removed 24 h after TZT-1027 administration, showing extensive central necrosis (N) and a rim of viable cells (V). Scale bars: 50 μm (**A** and **B**), 100 μm (**C**), and 200 μm (**D** and **E**).

TZT-1027 before irradiation induced a marked increase in the proportion of apoptotic cells compared with that apparent with radiation alone. These results thus suggested that potentiation of apoptosis contributed to radiosensitisation by TZT-1027.

Combined treatment with radiation and a single administration of TZT-1027 also inhibited the growth of tumours formed by H460 or A549 cells *in vivo* to a greater extent than did either treatment alone. Tumour microenvironmental factors, such as the vascular supply, are important determinants of sensitivity to radiation therapy *in vivo*. The ability of microtubule-targeting agents to induce a rapid shutdown of the existing tumour vasculature has been recognised by their designation as vascular-targeting agents (VTAs) (Jordan and Wilson, 2004). Treatment with VTAs such as ZD6126 and combretastatin A-4-P typically results in the destruction of large areas of a tumour, with surviving cells remaining only at the tumour periphery (Dark *et al*, 1997; Blakey *et al*, 2002). These peripheral viable tumour cells presumably derive their nutritional support from nearby normal blood vessels that are not responsive to VTA treatment (Li *et al*, 1998; Siemann and Rojiani, 2002). Such support together with a rapid upregulation of angiogenic factors such as vascular endothelial growth factor may directly facilitate the growth and expansion of the remaining tumour cells (Wachsberger *et al*, 2003; Thorpe, 2004). Given that these residual tumour cells are likely well oxygenated (Wachsberger *et al*, 2003), they are an ideal target for radiation therapy. Several studies have recently shown that treatment with VTAs enhances the therapeutic effect of radiotherapy (Li *et al*, 1998; Siemann and Rojiani, 2002, 2005; Horsman and Murata, 2003; Masunaga *et al*, 2004), consistent with the idea that the components of such combination therapy act in a complementary manner, with VTAs attacking the poorly oxygenated cell population in the central region of tumours and radiation killing the well-oxygenated proliferating cells at the tumour periphery (Li *et al*, 1998; Siemann and Rojiani, 2002; Wachsberger *et al*, 2003). TZT-1027 was previously shown to increase vascular permeability and to induce a decrease in tumour blood flow followed by a marked increase in tissue necrosis in the central region of tumour xenografts (Otani *et al*, 2000; Watanabe *et al*, 2006b). We have now shown that TZT-1027 treatment resulted in congestion and occlusion of tumour blood vessels followed by extensive necrosis of the tumour core, with only a thin rim of viable tumour cells remaining, in the H460 tumour model, suggesting that TZT-1027 acts as a VTA. The action of TZT-1027 as a VTA might thus contribute to the radiosensitising effect observed *in vivo* in the present study.

The clinical use of microtubule-interfering agents such as taxanes in combination with radiation has been successful in improving local tumour control. However, taxanes are often of limited efficacy because of the development of cellular resistance such as that mediated by P-glycoprotein-dependent drug efflux (Goodin *et al*, 2004). The action of TZT-1027 has been suggested to be less affected by multidrug resistance factors, including overexpression of P-glycoprotein, than that of other tubulin inhibitors (Watanabe *et al*, 2006a), suggesting that TZT-1027 may be effective in the treatment of taxane-refractory tumours. Further investigations are thus warranted to examine the combined effects of TZT-1027 and ionising radiation on drug-resistant tumour cells. Whether TZT-1027 enhances the tumour response to clinically relevant fractionated doses of radiation such as 2 Gy per fraction also warrants further study.

In conclusion, we have found that the inhibitory effect of TZT-1027 on cell cycle progression is highly specific to M phase. Moreover, TZT-1027 enhanced the effects of radiation on human cancer cells both *in vitro* and in animal models *in vivo*. These preclinical results provide a rationale for future clinical investigations of the therapeutic efficacy of TZT-1027 in combination with radiotherapy.

ACKNOWLEDGEMENTS

We thank H Kakeya for providing tsFT210 cells as well as M Kobayashi, T Natsume, E Hatashita, Y Yamada, and S Ono for technical assistance.

REFERENCES

Blakey DC, Westwood FR, Walker M, Hughes GD, Davis PD, Ashton SE, Ryan AJ (2002) Antitumor activity of the novel vascular targeting agent ZD6126 in a panel of tumor models. *Clin Cancer Res* **8**: 1974–1983

Choy H, Yee L, Cole BF (1995) Combined-modality therapy for advanced non-small cell lung cancer: paclitaxel and thoracic irradiation. *Semin Oncol* **22**: 38–44

Dark GG, Hill SA, Prise VE, Tozer GM, Pettit GR, Chaplin DJ (1997) Combretastatin A-4, an agent that displays potent and selective toxicity toward tumor vasculature. *Cancer Res* **57**: 1829–1834

de Jonge MJ, van der Gaast A, Planting AS, van Doorn L, Lems A, Boot I, Wanders J, Satomi M, Verweij J (2005) Phase I and pharmacokinetic study of the dolastatin 10 analogue TZT-1027, given on days 1 and 8 of a 3-week cycle in patients with advanced solid tumors. *Clin Cancer Res* **11**: 3806–3813

Edelstein MP, Wolfe III LA, Duch DS (1996) Potentiation of radiation therapy by vinorelbine (Navelbine) in non-small cell lung cancer. *Semin Oncol* **23**: 41–47

Goodin S, Kane MP, Rubin EH (2004) Epothilones: mechanism of action and biologic activity. *J Clin Oncol* **22**: 2015–2025

Greystoke A, Blagden S, Thomas AL, Scott E, Attard G, Molife R, Vidal L, Pacey S, Sarkar D, Jenner A, De-Bono JS, Steward W (2006) A phase I study of intravenous TZT-1027 administered on day 1 and day 8 of a three-weekly cycle in combination with carboplatin given on day 1 alone in patients with advanced solid tumours. *Ann Oncol* **17**: 1313–1319

Hofstetter B, Vuong V, Broggini-Tenzer A, Bodis S, Ciernik IF, Fabbro D, Wartmann M, Folkers G, Pruschy M (2005) Patupilone acts as radiosensitizing agent in multidrug-resistant cancer cells *in vitro* and *in vivo*. *Clin Cancer Res* **11**: 1588–1596

Horsman MR, Murata R (2003) Vascular targeting effects of ZD6126 in a C3H mouse mammary carcinoma and the enhancement of radiation response. *Int J Radiat Oncol Biol Phys* **57**: 1047–1055

Jordan MA, Wilson L (2004) Microtubules as a target for anticancer drugs. *Nat Rev Cancer* **4**: 253–265

Kim JC, Kim JS, Saha D, Cao Q, Shyr Y, Choy H (2003) Potential radiation-sensitizing effect of semisynthetic epothilone B in human lung cancer cells. *Radiother Oncol* **68**: 305–313

Kim JS, Amorino GP, Pyo H, Cao Q, Price JO, Choy H (2001) The novel taxane analogs, BMS-184476 and BMS-188797, potentiate the effects of radiation therapy *in vitro* and *in vivo* against human lung cancer cells. *Int J Radiat Oncol Biol Phys* **51**: 525–534

Kobayashi M, Natsume T, Tamaoki S, Watanabe J, Asano H, Mikami T, Miyasaka K, Miyazaki K, Gondo M, Sakakibara K, Tsukagoshi S (1997) Antitumor activity of TZT-1027, a novel dolastatin 10 derivative. *Jpn J Cancer Res* **88**: 316–327

Lawrence TS, Davis MA, Hough A, Rehemtulla A (2001) The role of apoptosis in 2′,2′-difluoro-2′-deoxycytidine (gemcitabine)-mediated radiosensitization. *Clin Cancer Res* **7**: 314–319

Li L, Rojiani A, Siemann DW (1998) Targeting the tumor vasculature with combretastatin A-4 disodium phosphate: effects on radiation therapy. *Int J Radiat Oncol Biol Phys* **42**: 899–903

Liebmann J, Cook JA, Fisher J, Teague D, Mitchell JB (1994) *In vitro* studies of Taxol as a radiation sensitizer in human tumor cells. *J Natl Cancer Inst* **86**: 441–446

Masunaga S, Sakurai Y, Suzuki M, Nagata K, Maruhashi A, Kinash Y, Ono K (2004) Combination of the vascular targeting agent ZD6126 with boron neutron capture therapy. *Int J Radiat Oncol Biol Phys* **60**: 920–927

Miyazaki K, Kobayashi M, Natsume T, Gondo M, Mikami T, Sakakibara K, Tsukagoshi S (1995) Synthesis and antitumor activity of novel dolastatin 10 analogs. *Chem Pharm Bull (Tokyo)* **43**: 1706–1718

Mollinedo F, Gajate C (2003) Microtubules, microtubule-interfering agents and apoptosis. *Apoptosis* **8**: 413–450

Natsume T, Watanabe J, Horiuchi T, Kobayashi M (2006) Combination effect of TZT-1027 (Soblidotin) with other anticancer drugs. *Anticancer Res* **26**: 1145–1151

Natsume T, Watanabe J, Koh Y, Fujio N, Ohe Y, Horiuchi T, Saijo N, Nishio K, Kobayashi M (2003) Antitumor activity of TZT-1027 (Soblidotin) against vascular endothelial growth factor-secreting human lung cancer *in vivo*. *Cancer Sci* **94**: 826–833

Natsume T, Watanabe J, Tamaoki S, Fujio N, Miyasaka K, Kobayashi M (2000) Characterization of the interaction of TZT-1027, a potent antitumor agent, with tubulin. *Jpn J Cancer Res* **91**: 737–747

Osada H, Cui CB, Onose R, Hanaoka F (1997) Screening of cell cycle inhibitors from microbial metabolites by a bioassay using a mouse cdc2 mutant cell line, tsFT210. *Bioorg Med Chem* **5**: 193–203

Otani M, Natsume T, Watanabe JI, Kobayashi M, Murakoshi M, Mikami T, Nakayama T (2000) TZT-1027, an antimicrotubule agent, attacks tumor vasculature and induces tumor cell death. *Jpn J Cancer Res* **91**: 837–844

Pawlik TM, Keyomarsi K (2004) Role of cell cycle in mediating sensitivity to radiotherapy. *Int J Radiat Oncol Biol Phys* **59**: 928–942

Schoffski P, Thate B, Beutel G, Bolte O, Otto D, Hofmann M, Ganser A, Jenner A, Cheverton P, Wanders J, Oguma T, Atsumi R, Satomi M (2004) Phase I and pharmacokinetic study of TZT-1027, a novel synthetic dolastatin 10 derivative, administered as a 1-hour intravenous infusion every 3 weeks in patients with advanced refractory cancer. *Ann Oncol* **15**: 671–679

Siemann DW, Rojiani AM (2002) Enhancement of radiation therapy by the novel vascular targeting agent ZD6126. *Int J Radiat Oncol Biol Phys* **53**: 164–171

Siemann DW, Rojiani AM (2005) The vascular disrupting agent ZD6126 shows increased antitumor efficacy and enhanced radiation response in large, advanced tumors. *Int J Radiat Oncol Biol Phys* **62**: 846–853

Simoens C, Vermorken JB, Korst AE, Pauwels B, De Pooter CM, Pattyn GG, Lambrechts HA, Breillout F, Lardon F (2006) Cell cycle effects of vinflunine, the most recent promising Vinca alkaloid, and its interaction with radiation, *in vitro*. *Cancer Chemother Pharmacol* **58**: 210–218

Sinclair WK (1968) Cyclic x-ray responses in mammalian cells *in vitro*. *Radiat Res* **33**: 620–643

Sinclair WK, Morton RA (1966) X-ray sensitivity during the cell generation cycle of cultured Chinese hamster cells. *Radiat Res* **29**: 450–474

Tamura K, Nakagawa K, Kurata T, Satoh T, Nogami T, Takeda K, Mitsuoka S, Yoshimura N, Kudoh S, Negoro S, Fukuoka M (2007) Phase I study of TZT-1027, a novel synthetic dolastatin 10 derivative and inhibitor of tubulin polymerization, which was administered to patients with advanced solid tumors on days 1 and 8 in 3-week courses. *Cancer Chemother Pharmacol* (in press)

Tamura K, Rice RL, Wipf P, Lazo JS (1999) Dual G_1 and G_2/M phase inhibition by SC-alpha alpha delta 9, a combinatorially derived Cdc25 phosphatase inhibitor. *Oncogene* **18**: 6989–6996

Thorpe PE (2004) Vascular targeting agents as cancer therapeutics. *Clin Cancer Res* **10**: 415–427

Vokes EE, Haraf DJ, Masters GA, Hoffman PC, Drinkard LC, Ferguson M, Olak J, Watson S, Golomb HM (1996) Vinorelbine (Navelbine), cisplatin, and concomitant radiation therapy for advanced malignancies of the chest: a Phase I study. *Semin Oncol* **23**: 48–52

Wachsberger P, Burd R, Dicker AP (2003) Tumor response to ionizing radiation combined with antiangiogenesis or vascular targeting agents: exploring mechanisms of interaction. *Clin Cancer Res* **9**: 1957–1971

Watanabe J, Minami M, Kobayashi M, Natsume T, Watanabe J, Horiuchi T, Kobayashi M (2006a) Antitumor activity of TZT-1027 (Soblidotin). *Anticancer Res* **26**: 1973–1981

Watanabe J, Natsume T, Fujio N, Miyasaka K, Kobayashi M (2000) Induction of apoptosis in human cancer cells by TZT-1027, an antimicrotubule agent. *Apoptosis* **5**: 345–353

Watanabe J, Natsume T, Kobayashi M (2006b) Antivascular effects of TZT-1027 (Soblidotin) on murine Colon26 adenocarcinoma. *Cancer Sci* **97**: 1410–1416

Workman P, Twentyman P, Balkwill F, Balmain A, Chaplin D, Double J, Embleton J, Newell D, Raymond R, Stables J, Stephens T, Wallace J (1998) United Kingdom Co-ordinating Committee on Cancer Research (UKCCCR) Guidelines for the Welfare of Animals in Experimental Neoplasia 2nd edn. *Br J Cancer* **77**: 1–10

切除不能局所進行非小細胞肺癌に対する分子標的治療の現状
―胸部放射線療法との併用―

引野幸司*　大江裕一郎*

要　旨

切除不能局所進行非小細胞肺癌に対する標準的治療は，現在のところシスプラチンを含む化学療法と同時胸部放射線療法であることがほぼコンセンサスとなっているが，まだまだ十分な治療成績とは言えない状況である．近年，分子標的薬が非小細胞肺癌の治療薬として注目され，放射線療法との併用で相乗効果も報告されている．これを踏まえ，切除不能局所進行非小細胞肺癌に対して分子標的薬と化学・胸部放射線療法を併用する臨床試験が行われている．今後のさらなる治療成績向上において，分子標的薬は非常に重要な治療戦略と言える．

はじめに

日本での肺癌による死亡者は年間約6万人に上り，癌による死亡原因の第1位となった．今後も肺癌の発生数，死亡者数は増加することが予想されている．Japan Clinical Oncology Group（JCOG）肺がん内科グループで施行された切除不能局所進行の非小細胞肺癌（NSCLC）に対する化学放射線療法の6つの臨床試験では，240 症例の生存期間中央値（MST）は16.1ヵ月，5年生存率14.4%であった[1]．まだまだ予後不良と言える肺癌の治療成績向上のためには，新しい治療戦略が必要とされる状況である．

* 国立がんセンター中央病院 肺内科

キーワード：局所進行非小細胞肺癌，分子標的薬，胸部放射線療法

切除不能局所進行非小細胞肺癌（NSCLC）の標準的治療

切除不能局所進行 NSCLC とは，ⅢA 期および胸水貯留例を除くⅢB 期で，根治手術が困難である NSCLC の総称である．以前は胸部放射線療法（TRT）が標準とされていたが，メタアナリシスの結果からシスプラチンを含む化学療法と TRT の併用が標準と考えられるようになった[2~4]．次に，TRT を行うタイミング，同時か逐次かを比較した第Ⅲ相臨床試験が行われるようになった．MST において同時群 15.0～17.0ヵ月 対 逐次群 13.3～14.4ヵ月という結果が得られ，標準的治療は化学療法と同時 TRT であることがほぼコ

ンセンサスとなってきた[1)4)]．一方，化学療法においてどのレジメンを用いるかについては第Ⅲ相試験もほとんどなく，確立されていない状況である．

国立がんセンター中央病院を中心に行われたシスプラチン＋ビノレルビン併用化学療法と同時 TRT の第Ⅰ相臨床試験では，奏効率 83% [95% 信頼区間（CI）59～96%]，MST は 30.4ヵ月，3年生存率は 50% であった[5)]．また Southwest Oncology Group（SWOG）は，シスプラチン＋エトポシドの化学療法と同時 TRT を行った後にドセタキセルの地固め療法を実施するという S9504 試験を行い，MST 26ヵ月，5年生存率 29% という結果であった[6)7)]．これを受けて国立がんセンター中央病院を中心に，シスプラチン＋ビノレルビンと同時 TRT 後にドセタキセルによる地固め療法を行う試験が行われた．ドセタキセルについては，地固め療法を行っている期間にグレード3～4の好中球減少，食道炎，肺臓炎といった毒性が問題となったが，奏効率 81.7%（95%CI 72.7～88.0%），MST 30.4ヵ月（95%CI 24.5～36.6），3年生存率 42.6% という結果が得られた[8)]．これらのデータから，日本では同時 TRT に併用する化学療法レジメンとしてはシスプラチン＋ビノレルビンが比較的多く用いられていると考えられる．

EGFR チロシンキナーゼ阻害薬と胸部放射線療法（TRT）の併用

EGF 受容体（EGFR）のチロシンキナーゼ阻害薬であるゲフィチニブ（イレッサ®，ZD1839）は，既治療 NSCLC を対象とした第Ⅱ相臨床試験において，日本人で奏効率 27.5% であった[9)]．また *in vivo* の実験では，ゲフィチニブとエルロチニブ（タルセバ®，OSI-774）には放射線との相乗効果が報告されている[10)]．頭頸部扁平上皮癌において，放射線療法単独群と放射線に EGFR に対するモノクローナル抗体であるセツキシマブ（cetuximab，C225）を併用する群を比較する第Ⅲ相臨床試験では，MST は単独群 29.3ヵ月対併用群 49.0ヵ月，3年生存率は単独群 45% 対併用群 55% という結果であった（p＝0.03）[11)]．これらのことから，放射線療法に EGFR チロシンキナーゼ阻害薬を併用することで，局所進行 NSCLC の治療成績にも改善がもたらされることが期待されるようになった．

Rischin は，15 例の NSCLC 患者に対してカルボプラチン＋パクリタキセルと同時 TRT にゲフィチニブを併用する第Ⅰ相臨床試験を行い，奏効率 91% という結果を報告した[12)]．Ready はⅢ期 NSCLC に対してカルボプラチン＋パクリタキセルにゲフィチニブを併用し，TRT を同時群と遂次群に分けた第Ⅱ相臨床試験を行ったが，肺毒性の増強は認められなかった[13)]．SWOG では S9504 の結果を踏まえ，シスプラチン＋エトポシドと同時 TRT を行い，次いでドセタキセルを投与した後にゲフィチニブを追加する群とプラセボ群に割り付ける第Ⅲ相臨床試験（S0023）を施行した（図1）．この試験の目的は NSCLC におけるゲフィチニブ維持療法の有用性を検討することであったが，INTACT（IRESSA NSCLC Trial Assessing Combination Treatment）や ISEL（IRESSA Survival Evaluation in Lung Cancer）でゲフィチニブの延命効果が証明できなかったという結果を受けて早期中間解析を行ったところ，無増悪期間，MST ともに統計学的には有意差を認めなかったものの，試験を継続してもゲフィチニブによる延命効果は期待できないと結論づけられ，試験中止となっている[14)]．2007 年の米国臨床腫瘍学会（ASCO）にて，MST はゲフィチニブ群 23ヵ月対プラセボ群 35ヵ月（p＝0.013）という，その後の経過観察（平均 27ヵ月）のデータが発表されている[15)]．